Gravitational lensing as signal and noise in Lyman-α forest measurements

Marilena LoVerde,[1,2,*] Stefanos Marnerides,[2,†] Lam Hui,[1,2,3,‡] Brice Ménard,[4,§] and Adam Lidz[5,6,‖]

[1]*Institute for Advanced Study, Princeton, New Jersey 08540, USA*
[2]*ISCAP and Department of Physics, Columbia University, New York, New York 10027, USA*
[3]*CCPP and Department of Physics, New York University, New York 10003, USA*
[4]*Canadian Institute for Theoretical Astrophysics, Toronto, Ontario M5S 3H8, Canada*
[5]*Center for Astrophysics, Harvard University, Cambridge, Massachusetts 02138, USA*
[6]*Department of Physics and Astronomy, University of Pennsylvania, Philadelphia, Pennsylvania 19104, USA*

(Received 15 April 2010; published 5 November 2010)

In Lyman-α forest measurements it is generally assumed that quasars are mere background light sources which are uncorrelated with the forest. Gravitational lensing of the quasars violates this assumption. This effect leads to a measurement bias, but more interestingly it provides a valuable signal. The lensing signal can be extracted by correlating quasar magnitudes with the flux-power spectrum and with the flux decrement. These correlations will be challenging to measure but their detection provides a *direct* measure of how features in the Lyman-α forest trace the underlying mass density field. Observing them will test the fundamental hypothesis that fluctuations in the forest are predominantly driven by fluctuations in mass, rather than in the ionizing background, helium reionization, or winds. We discuss ways to disentangle the lensing signal from other sources of such correlations, including dust, continuum, and background residuals. The lensing-induced measurement bias arises from sample selection: one preferentially collects spectra of magnified quasars which are behind overdense regions. This measurement bias is $\sim$0.1–1% for the flux-power spectrum, optical depth, and the flux probability distribution. Since the effect is systematic, quantities such as the amplitude of the flux-power spectrum averaged across scales should be interpreted with care.

DOI: 10.1103/PhysRevD.82.103507 PACS numbers: 98.80.Es, 95.35.+d, 98.65.Dx

I. INTRODUCTION

Light from distant galaxies and quasars is gravitationally lensed by mass along the line of sight. For a flux-limited survey of quasars, lensing magnification biases the observed number density [1–3]. For example, a positive mass fluctuation along the line of sight can increase the apparent sky area and the observed flux. The geometrical area increase decreases the quasar number density, while the flux increase promotes intrinsically faint objects above the magnitude threshold increasing the source density. Together these effects introduce a correction to the quasar number density called magnification bias. Detections of the magnification of distant quasars by low-redshift galaxies confirm the presence of this effect (e.g. [4–6]).

Many authors have studied the effect of lensing magnification on observations of the galaxy correlation function and power spectrum. Another way of inferring the large-scale mass distribution is through measurements of the neutral Hydrogen density. As light from distant quasars passes through clouds of neutral Hydrogen, photons with rest-frame frequency at the Lyman-α transition (1216 Å) are absorbed. The observed quasar spectrum contains troughs corresponding to absorption by neutral Hydrogen at redshift $z = \nu_\alpha/(\nu_{\rm obs}(1 + v_{\rm pec})) - 1$, where $\nu_{\rm obs}$ is the observed frequency of the trough, $v_{\rm pec}$ is the peculiar velocity at z (speed of light is set to unity), and ν_α is the Lyman-α frequency.[1] This Lyman-α forest (of absorption features in the quasar spectrum) is a cosmological tool that can be used to probe the neutral Hydrogen along the line of sight (see for example [7] and references therein). Here we ask two questions: what is the effect of gravitational lensing on measurements of the Lyman-α forest? And how can we extract the gravitational signal from such measurements?

Let us first discuss qualitatively what we expect to happen. Consider a single line of sight towards a quasar at comoving distance χ_Q. Lensing magnification changes the observed quasar flux f, but in a frequency (ν) independent way

$$f(\nu) \to f(\nu) \cdot \mu(\chi_Q), \tag{1}$$

where $\mu(\chi_Q)$ is the magnification which depends on the density fluctuations along the line of sight. Since all frequencies are treated in the same way, fluctuations in the flux as a function of frequency are *unaffected*—just as if we were looking at an intrinsically brighter or dimmer quasar.

*marilena@ias.edu
†stefanos@phys.columbia.edu
‡lhui@astro.columbia.edu
§menard@cita.utoronto.ca
‖alidz@sas.upenn.edu

[1]Here, the redshift z refers to the intrinsic or cosmological redshift, i.e. the redshift if the absorbing materials were comoving. The observed redshift and the intrinsic redshift are related by $1 + z_{\rm obs} = (1 + z)(1 + v_{\rm pec})$.

Measurements of, for example, the flux-power spectrum, from an *individual* line of sight are unchanged by magnification. On the other hand, magnification does change *which* lines of sight are observed. More precisely, a selection bias is introduced: more (fewer) quasars are observed along lines of sight that lead to a positive (negative) magnification correction to quasar number counts. Let $n(\chi, \boldsymbol{\theta})$ be the number density of quasars at comoving distance χ in direction $\boldsymbol{\theta}$. Under the effect of lensing magnification,

$$n(\chi, \boldsymbol{\theta}) \rightarrow n(\chi, \boldsymbol{\theta})\mu(\chi)^{2.5s-1},$$
$$s = \frac{1}{\ln 10}\frac{\int dm \epsilon(m)(dn^0/dm)}{\int dm \epsilon(m) n^0(m)}. \quad (2)$$

Here, $n^0(m)$ is the luminosity function of quasars at magnitude m (i.e. $dmn^0(m)$ is the number density of quasars at magnitude $m \pm dm/2$), and $\epsilon(m)$ quantifies the sample definition—the simplest example is a step function which cuts off all quasars fainter than some limiting magnitude $m_{\rm lim}$, in which case s reduces to the more familiar expression $s = d\log_{10}N(<m_{\rm lim})/dm_{\rm lim}$, where $N(<m_{\rm lim})$ is the total number of quasars brighter than $m_{\rm lim}$. This is a well-known result, but a derivation is summarized in Appendix A. With lensing magnification, the lines of sight we observe do not constitute a fair sample of the density field. Therefore, while lensing magnification has *no* effect on measurements of the flux fluctuation from a *single* quasar line of sight, measurements dependent upon the density field *averaged over multiple quasars will* be biased. This occurs since the observable (e.g. the neutral hydrogen density) is correlated with the magnification which depends on the gravitational potential along the line of sight.

What is perhaps the more interesting question is how we could extract the lensing signal from observations of the forest. The discussions above make clear gravitational lensing affects both the observed brightness and number density of quasars. One could imagine cross correlating these quantities with the Lyman-α forest observables. We will consider several possibilities and identify the ones with an interesting signal to noise.

The rest of the paper is organized as follows. In Sec. II A we develop a simple description of the effect of lensing magnification on measurements of the Lyman-α forest, the key result is Eq. (8). In Sec. II B, II C, II D, and II E we present the effect of lensing bias on the flux-power spectrum, the effective optical depth and the flux probability distribution (PDF) determined by applying a biased weighting scheme to mock absorption spectra from simulations and compare these results with analytical estimates in terms of the flux-mass polyspectra. In Sec. III we discuss the exciting possibility of observing the lensing-induced correlation between quasar magnitudes and the flux fluctuations, the flux-power spectrum or the mean flux. While this work is dedicated to discussing magnification bias, dust along the line of sight would have a similar (though generally opposite signed) effect, this is discussed in Sec. III E. We present concluding remarks and discuss the implications of this work for existing and future Lyman-α measurements in Sec. IV. Appendix A contains a unified derivation of the magnitude-forest correlations and the lensing bias discussed in the paper. In Appendix B we discuss some issues regarding large-scale flux-mass correlations measured from our simulations and the accuracy of an analytic description. Appendix C derives an estimator for the flux-magnitude correlation and its associated error.

Before proceeding we should mention some related literature. The magnification bias to the statistics of metal absorption lines in quasar spectra was investigated in [8], and a method for detecting statistical lensing by absorbers was proposed in [9]. Lensing effects on the statistics of damped Lyman-α systems and the inferred density of neutral Hydrogen were considered in [10]. More recently, [11] studied magnification bias due to intervening absorbers in the 2dF quasar survey and [12] in the Sloan Digital Sky Survey (SDSS). Recent work by [13,14] proposed correlating lensing in the cosmic microwave background with fluctuations in the forest to extract the flux-mass correlation.

II. LENSING AS NOISE/BIAS

A. Formalism

We are interested in some Lyman-α forest observable $\mathcal{O}$, which can represent the flux-power spectrum, the flux transmission/decrement, the flux fluctuation (around its mean), and so on. Let us use O_I to denote the observable measured from a quasar labeled by I. We typically form an estimator by averaging over quasars:

$$\mathcal{O}_{\rm obs} = \frac{\sum_I w_I \mathcal{O}_I}{\sum_I w_I}, \quad (3)$$

where w_I denotes weights, the simplest example of which is $w_I = 1$.

Two important points. First $\mathcal{O}_I$, the observable on a quasar by quasar basis, is generally *not* affected by gravitational lensing. This is because gravitational lensing affects all wavelengths equally. For instance, $\mathcal{O}_I$ could represent the flux transmission which is f/f_C (where f and f_C are the flux and continuum, respectively, as a function of frequency), or the flux fluctuation $\delta_f = (f - \bar{f})/\bar{f}$ (where $\bar{f}$ is the flux averaged for the particular line of sight in question). Since gravitational lensing brightens or dims f, $\bar{f}$, and f_C all equally independent of wavelength, there is no effect on $\mathcal{O}_I$.

The other important point is that $\mathcal{O}_{\rm obs}$ *is* generally affected by lensing. The crucial observation is that w_I in Eq. (3) reveals only part of the weighting that is going on; in any given data set, we inevitably give zero weights to quasars which are too faint to observe. This means that

even if one chooses $w_I = 1$, one is merely performing a straight average over one's sample, as opposed to an average over all possible quasars. To account for this fact, it is helpful to pixelize the sky, and rewrite $\mathcal{O}_{\rm obs}$ as

$$\mathcal{O}_{\rm obs} = \frac{\sum_i w_i n_i \mathcal{O}_i}{\sum_i w_i n_i}, \tag{4}$$

where i is the pixel label. One could conceptually think of each pixel as sufficiently small that the number of quasars in it n_i is either 1 or 0; we will more generally think of n_i as simply the number density of quasars in pixel i. This way of rewriting is useful because it makes explicit the fact that $\mathcal{O}_{\rm obs}$ is a weighted average—it is weighted by the number density of quasars, on top of whatever additional weighting w_i one might wish to apply. In other words, since our Lyman-α forest observable can be measured only if there exists a background quasar in the sky location of interest, the observable is always implicitly weighted by the abundance of quasars.

Equation (2) tells us that

$$n_i = n_i^{\rm intrinsic}(1 + \delta_i^\mu), \tag{5}$$

where $n_i^{\rm intrinsic}$ is the intrinsic pre-lensed quasar number density, and δ_i^μ is the lensing modification given by

$$\begin{aligned} \delta_i^\mu &\equiv (5s - 2)\kappa_i, \\ \kappa_i &= \int_0^{\chi_Q} d\chi' \frac{\chi_Q - \chi'}{\chi_Q} \chi' \nabla_\perp^2 \phi(\chi', i), \end{aligned} \tag{6}$$

assuming fluctuations are small. The expression for the convergence κ_i assumes spatial flatness, but can be easily generalized to nonflat universes (χ_Q is the comoving distance to quasar). Here, $1 + 2\kappa$ is the weak lensing approximation to the lensing magnification μ of Eqs. (1) and (2) [the full nonlinear expression is given in footnote 7]. Using $w_i = 1$ in Eq. (4), assuming there is no correlation between the forest observable and the intrinsic quasar number fluctuation, and ignoring corrections of the integral constraint type (see Appendix A and, for example, [15]), we obtain the following ensemble average, to the lowest order in fluctuations:

$$\langle \mathcal{O}_{\rm obs} \rangle = \mathcal{O}_{\rm true} + \langle \mathcal{O}_i \delta_i^\mu \rangle, \tag{7}$$

where $\langle \mathcal{O}_i \delta_i^\mu \rangle$ is the correlation between the observable and the magnification fluctuation at the same i (i.e. zero lag). Dropping the i label, the lensing-induced measurement bias on an observable $\mathcal{O}$ is therefore

$$\langle \mathcal{O}_{\rm obs} \rangle - \mathcal{O}_{\rm true} = \langle \mathcal{O}\delta^\mu \rangle = (5s - 2)\langle \mathcal{O}\kappa \rangle. \tag{8}$$

This is a fundamental expression that we will use repeatedly below. The meaning of each of these symbols is as follows: $\mathcal{O}$ is the fluctuation which we attempt to measure with the estimator $\mathcal{O}_{\rm obs}$, which upon ensemble averaging generally differs from the true underlying value $\mathcal{O}_{\rm true} = \langle \mathcal{O} \rangle$.

It is important to emphasize the actual measurement bias could be different. The above estimate assumes that all quasars *within one's sample* are weighted equally (i.e. $w_i = 1$). In practice, one might want to weigh brighter quasars *within one's sample* more strongly. For instance, one could weigh by the net flux of the quasar, which corresponds to inverse variance weighting in the noise dominated regime. This would result in a lensing-induced measurement bias of (see Appendix A for derivation)

$$\langle \mathcal{O}_{\rm obs} \rangle - \mathcal{O}_{\rm true} = (5s' - 2)\langle \mathcal{O}\kappa \rangle, \tag{9}$$

where s' is defined as

$$s' = \frac{1}{\ln 10} \frac{\int dm \epsilon(m)(dn^0/dm)10^{-m/2.5}}{\int dm \epsilon(m) n^0(m) 10^{-m/2.5}}, \tag{10}$$

which can be contrasted with s defined in Eq. (2). For a step function sample definition ϵ, s' reduces to $d\log_{10}N'(<m_{\rm lim})/dm_{\rm lim} + 0.4$, where $N' = \int_{-\infty}^{m_{\rm lim}} dm n^0 10^{-m/2.5}$. This is generally larger than s.

The precise value of s or s' is sample dependent. The relatively low redshift ($1 < z < 2.2$) SDSS quasars that were used to measure the magnification-galaxy cross correlation have a slope that spans $-1 \lesssim 5s - 2 \lesssim 1.9$, depending on the magnitude cut [5]. For this paper, the higher redshift quasars for which the Lyman-α forest falls within the SDSS spectral range are more relevant. In Fig. 8 (in Appendix A) we show the cumulated number counts and rough estimates of s and s' from SDSS data release 6.

In the rest of this paper, we will adopt $s = 1$ (or $s' = 1$), so our results for the lensing biases can be scaled up and down by $(5s - 2)/3$ or $(5s' - 2)/3$.

We will also adopt the following set of cosmological parameters in presenting numerical estimates. We assume a flat ΛCDM cosmology with cosmological parameter values $\Omega_m = 0.3$, $\Omega_\Lambda = 0.7$, $\Omega_b = 0.04$ for the fractional densities in matter, vacuum and baryons; scalar spectral index $n_s = 1$; Hubble parameter today $H_0 = 100h$ km/s/Mpc with $h = 0.7$ and fluctuation amplitude $\sigma_8 = 0.9$. The speed of light is set to unity. In a few places we use analytic calculations of the matter and baryon power spectra. The 3D matter power spectrum is calculated using the transfer function of [16] with a modified shape parameter $\Gamma = \Omega_m h \exp[-\Omega_b(1 + \sqrt{2h}/\Omega_m)]$ [17], and the nonlinear evolution is modeled according to [18]. To relate baryons to mass we assume the 3D Fourier space fluctuations are related by $\delta_b(\mathbf{k}) = \exp[-k^2/k_s^2]\delta(\mathbf{k})$, where $k_s = k_J\sqrt{10/3}$ and k_J is the Jeans scale (see Appendix B for more details).

B. Lensing bias from simulations

Lensing magnification biases measurements of the forest so long as the forest observable is correlated with the lensing convergence [Eq. (8)]. Since features in the Lyman-α forest are caused by absorption by gas which

itself traces gravitational potentials, there ought to be a correlation between absorption features and the lensing convergence. However, the mapping between absorption-induced fluctuations in the flux and the gravitational potential is nonlinear and dependent on potentially uncertain physics, such as fluctuations in the ionizing background. For this reason we need to appeal to simulations to quantify the correlation between forest observables (e.g. δ_f and P_{ff}) and the lensing convergence.

In this section we use hydrodynamic simulations to study the effect of magnification bias on the Lyman-α forest. Specifically, we study the "D5" simulation of [19]. This simulation was run using an entropy-conserving [20] version of the smoothed particle hydrodynamics code GADGET [21]. It tracks 324^3 dark matter particles and 324^3 gas particles in a simulation volume of comoving side length $L = 33.75\ \mathrm{Mpc}/h$, and includes a subresolution model for star formation [22] and heating by a uniform background radiation field [23]. Further details regarding the simulation can be found in [19]. We generate mock Lyman-α forest spectra along random lines of sight through the simulation volume in the usual way, integrating through the smoothed particle hydrodynamics kernels of the particles, and incorporating the effect of peculiar velocities and thermal broadening (e.g. [24]). We generate mock spectra from simulation snapshots at $z = 2$, 3 ,and 4. In each case, we adjust the amplitude of the photo-ionizing background in the simulation to match the observed mean transmitted flux from [25]. We also make use of the "G6" simulation (see [26]), which tracks 2×486^3 particles in a $L = 100\ \mathrm{Mpc}/h$ box, in order to check the sensitivity of our results to finite box-size effects in Appendix B. We have checked that the flux-power spectra from these simulations approximately match the existing measurements.

Magnification bias biases which lines of sight an observer will see: sight lines with positive fluctuations in magnification are more abundant and those with negative less abundant. With simulations we can of course see every line of sight (a mock spectrum is generated regardless of whether there is a quasar behind it) so we mimic lensing bias by weighting each line of sight $\boldsymbol{\theta}$ by $1 + \delta^{\mu}(\boldsymbol{\theta})$. The simulations are in boxes of size $33.75\ \mathrm{Mpc}/h$, so we cannot actually calculate the lensing convergence κ along the entire line of sight but instead for the weighting of absorption measurements at redshift $\bar{z}$, we use[2]

$$w_{\boldsymbol{\theta}} = 1 + \delta^{\mu}(\boldsymbol{\theta}) \sim 1 + \frac{3}{2} H_0^2 \Omega_m (5s - 2) \times \frac{\chi_Q - \bar{\chi}}{\chi_Q} \bar{\chi}(1 + \bar{z}) \int_{\bar{\chi}}^{\bar{\chi}+L} d\chi' \delta(\chi', \boldsymbol{\theta}), \quad (11)$$

where L is the length of the box $\bar{\chi} = \chi(\bar{z})$, χ_Q is the distance to the quasar, δ is the mass fluctuation, and we have used the approximation $\nabla_{\perp}^2 \phi \approx \nabla^2 \phi = \frac{3}{2} H_0^2 \Omega_m (1 + z)\delta$ which should be valid under the line-of-sight integral. Since the bias only comes from the mass fluctuations δ which are correlated with flux fluctuations δ_f at the redshift we are considering, and correlations drop off rapidly with increased spatial separation, neglecting contributions to κ from mass fluctuations at lower redshifts should not be a bad approximation. We will verify this below by comparing the lensing bias thus obtained with that obtained from another method.

C. Bias to the flux-power spectrum

In panel (a) of Fig. 1 we show the 1D flux-power spectrum

$$P_{ff}(k_{\parallel}) = \frac{1}{L} |\delta(k_{\parallel})|^2 \quad (12)$$

measured from simulations.[3] In panels (b)–(d) we show the fractional correction due to magnification, calculated by weighting lines of sight by $1 + \delta_{\mu}$. Magnification weighs lines of sight with large κ more heavily than those with low κ. Measurements of δ_f at redshift $\bar{z}$ can be taken from quasars at redshift z_Q for $\bar{z} \lesssim z_Q \lesssim (1 + \bar{z})\nu_{\beta}/\nu_{\alpha} - 1$. The upper limit is set by where the Lyman-β line ($\lambda_{\beta} = 1026$ Å) can be confused with Lyman-α. The lensing weight function is peaked at $\chi \sim \chi_Q/2$, so for quasars at higher redshift, $\chi(\bar{z})$ is closer to the peak of the lensing weight function making the lensing correction larger than it is for quasars just beyond $\bar{z}$.

Magnification causes a $\lesssim 1\%$ change to P_{ff} with larger changes occurring at lower redshifts. The results shown in Fig. 1 assume $s = 1$ and that all quasars within one's sample are weighed equally. The actual lensing correction in realistic surveys could differ by factor of a few. The current statistical error on the amplitude of P_{ff}, averaged over scales, is $\sim 0.6\%$ from SDSS [27], which is a bit larger than the magnification correction shown in Fig. 1. However, as precision improves, a systematic offset such as that introduced by lensing could well be relevant.

It is instructive to get an analytic estimate for the bias to the flux-power spectrum. Equation (8) tells us the lensing bias for the flux-power spectrum is

$$\langle P_{ff\mathrm{obs}}(k_{\parallel}) \rangle - P_{ff\mathrm{true}}(k_{\parallel}) = \frac{1}{\Delta\chi} \langle \delta_f(k_{\parallel}) \delta_f^*(k_{\parallel}) \delta^{\mu} \rangle, \quad (13)$$

where $\Delta\chi$ is the length of the quasar spectra from which the power is measured. It is therefore clear that this lensing bias depends on the three-point function or bispectrum. Expressing δ^{μ} as a line-of-sight integral of the mass fluctuation [Eq. (11)], and judiciously applying the Limber's approximation [28,29], we obtain

[2]While it would be more accurate to leave the χ terms inside the integral, their amplitude is slowly varying across the length of our simulations box so Eq. (11) should not be a bad approximation.

[3]Our Fourier convention is $\delta(\mathbf{k}) = \int d^3\mathbf{x} e^{-i\mathbf{k}\cdot\mathbf{x}} \delta(\mathbf{x})$.

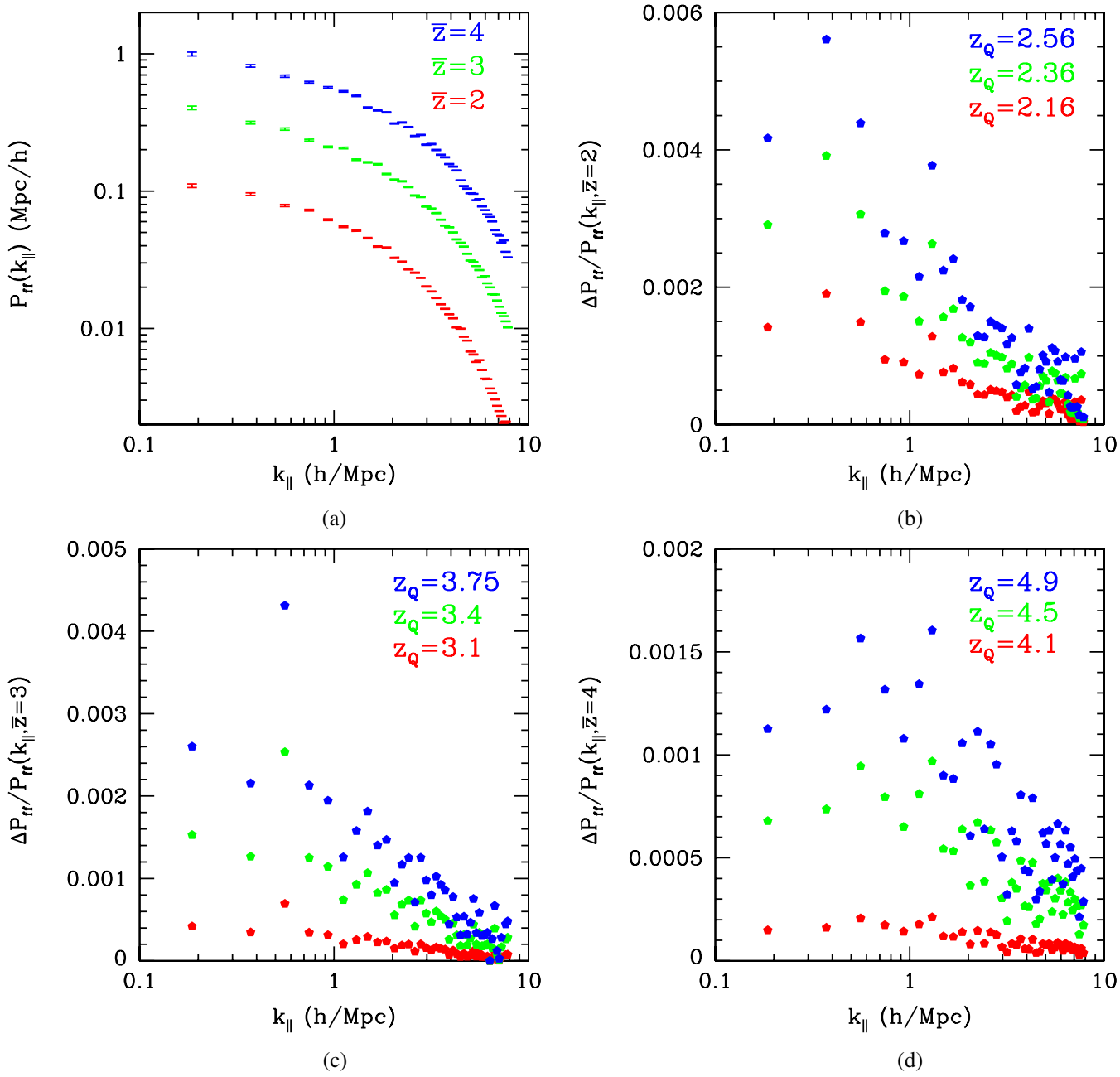

FIG. 1 (color online). (a) The 1D flux-power spectrum measured from the simulations. Panels (b)–(d) show the fractional correction from magnification $(\langle P_{ff\mathrm{obs}}\rangle - P_{ff\mathrm{true}})/P_{ff\mathrm{true}}$ for mean redshifts $\bar{z} = 2, 3, 4$, respectively. The error bars are suppressed for clarity. The amplitude of the correction depends on the redshift of the quasar z_Q through κ [Eq. (6)] and also on the slope of the quasar number count function, here we assume $5s - 2 = 3$.

$$\langle P_{ff\mathrm{obs}}(k_\parallel)\rangle - P_{ff\mathrm{true}}(k_\parallel) \approx \frac{3}{2}H_0^2\Omega_m(5s-2)\frac{\chi_Q - \bar{\chi}}{\chi_Q} \times \bar{\chi}(1+\bar{z})B_{ffm}(k_\parallel, -k_\parallel, 0), \tag{14}$$

where χ_Q is the distance to quasar, $\bar{\chi}$ is the average distance to the forest, and $\bar{z}$ is the corresponding redshift. Here, B_{ffm} is the (true) 1D flux-flux-mass bispectrum at redshift $\bar{z}$. It should be emphasized that $B_{ffm}(k_\parallel, -k_\parallel, 0)$ does not vanish despite having one of its arguments (the one associated with mass) being zero. This is related to the fact that it arises from a 1D projection of a 3D distribution. For instance, it is well known that a 3D power spectrum and its 1D projection are related by $P_{1D}(k_\parallel) = \int_{k_\parallel}^{\infty}(kdk/2\pi)P_{3D}(k)$, and so P_{1D} generally does not vanish in the $k_\parallel \to 0$ limit.

We calculate the correction to P_{ff} using B_{ffm} measured from simulations. Estimating $B_{ffm}(k_\parallel, -k_\parallel, 0)$ requires an extrapolation from what we actually measure $B_{ffm}(k_\parallel, -(k_\parallel + \Delta k), \Delta k)$, where the smallest Δk is the fundamental mode of the box. How this is done is described in detail in Appendix B. In Fig. 2 we compare the lensing correction to the flux-power spectrum as determined via the bispectrum to that determined by the weighting method described previously in Sec. II B. The qualitative agreement between the two is reassuring.

D. Bias to the effective optical depth

The effective optical depth $\tau_{\rm eff}$ is estimated from data by averaging over frequencies (and quasars) the ratio of the observed flux $f =$ to the continuum f_C, i.e. $e^{-\tau_{\rm eff}}$ is estimated from f/f_C. As emphasized in Sec. II A, lensing magnification affects f and f_C in the same manner, and therefore leaves f/f_C unchanged on a quasar by quasar basis. Lensing's impact enters through the sample selection, resulting in [see Eq. (8)]

$$\langle e^{-\tau_{\rm eff}}_{\rm obs}\rangle - e^{-\tau_{\rm eff}}_{\rm true} = \langle e^{-\tau_{\rm eff}}\delta^\mu\rangle, \tag{15}$$

where $e^{-\tau_{\rm eff}}$ on the right is the mean transmission on a line-of-sight by line-of-sight basis, and $e^{-\tau_{\rm eff}}_{\rm true}$ is the true mean transmission if only we could dispense with the quasar weighting and average over the whole sky equally.

The correction to the effective optical depth measured from simulations is shown in Fig. 3 for quasars at several redshifts. The net effect of lensing will depend on how measurements from quasars at different redshifts are combined. However, Fig. 3 indicates the effect should be $\sim 10^{-3} - 10^{-4}$. Current measurements of $\tau_{\rm eff}$ have errors of at least a few percent at each redshift so at present lensing should not be an issue.[4]

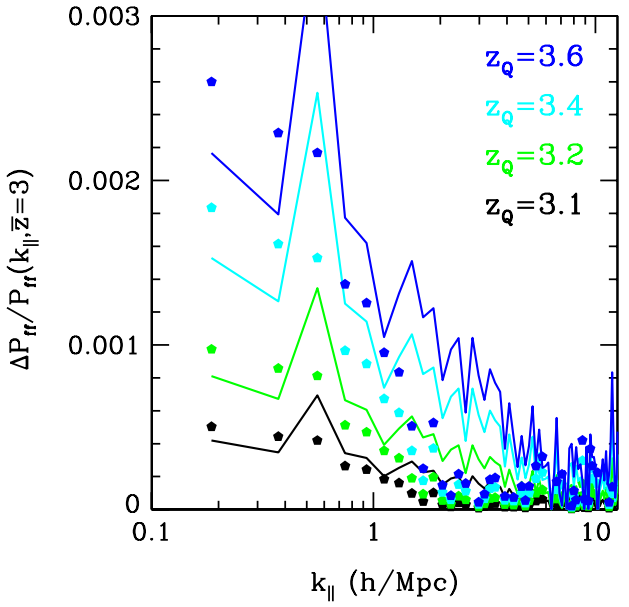

FIG. 2 (color online). A comparison of the predicted lensing bias to the flux-power spectrum using the weighted calculation presented in Sec. II B (solid lines) versus using Eq. (14) with the flux-flux-mass bispectrum measured from simulations (points). From bottom to top the quasar redshifts are 3.1, 3.2, 3.4, 3.6.

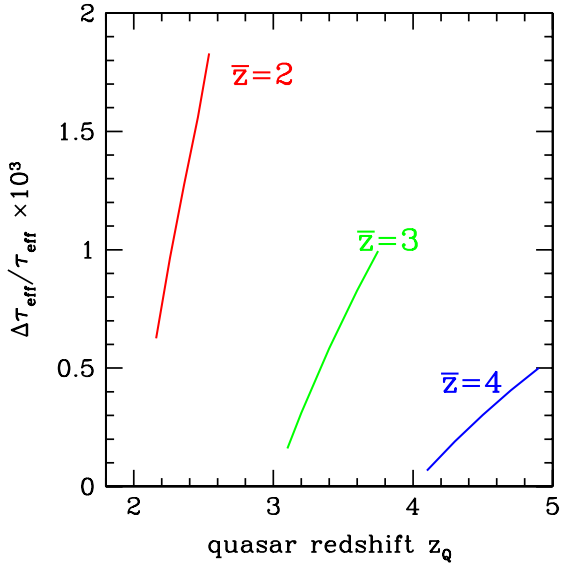

FIG. 3 (color online). The magnification correction to the effective optical depth at three different mean redshifts $\bar{z}$. This correction depends on the redshift z_Q of the quasars. In practice, measurements of $\tau_{\rm eff}$ involves combining source quasars at multiple redshifts. In the above plot we assume $5s - 2 = 3$.

An analytical estimate of the lensing bias on the effective optical depth can be inferred from Eq. (15), which gives

$$\frac{\langle e^{-\tau_{\rm eff}}{}_{\rm obs}\rangle}{e^{-\tau_{\rm eff}}{}_{\rm true}} - 1 = \langle \delta_f \delta^\mu\rangle \approx (5s-2)\frac{3}{2}\Omega_m H_0^2 \frac{\chi_Q - \bar{\chi}}{\chi_Q}\bar{\chi}(1+\bar{z}) \times P_{fm}(k_\parallel = 0), \tag{16}$$

where we have used Limber's approximation, $P_{fm}(k_\parallel)$ is the (true) 1D flux-mass power spectrum evaluated at the mean redshift of absorption $\bar{z}$, $\bar{\chi}$ is the corresponding distance, and χ_Q is the quasar distance. The lensing bias

[4]The error bars for measurements of $\tau_{\rm eff}$ are dominated by uncertainties in the continuum-fit. Typically, the continuum is estimated either by extrapolating from the red side (e.g. [30]), or by performing a smooth fit through portions of the spectra that are deemed unabsorbed (e.g. [25]). We simulate the effect of the latter by renormalizing the flux along each line of sight by $f_{\rm max}$, the maximum along that line of sight. At low redshifts, this introduces a negligible bias to $\tau_{\rm eff}$, but by $z = 4$, $\tau_{\rm eff}$ is biased low by $\sim 8\%$, in rough agreement with [25]. However, we have checked that the fractional magnification correction is not significantly changed whether we renormalize by $f_{\rm max}$ or not.

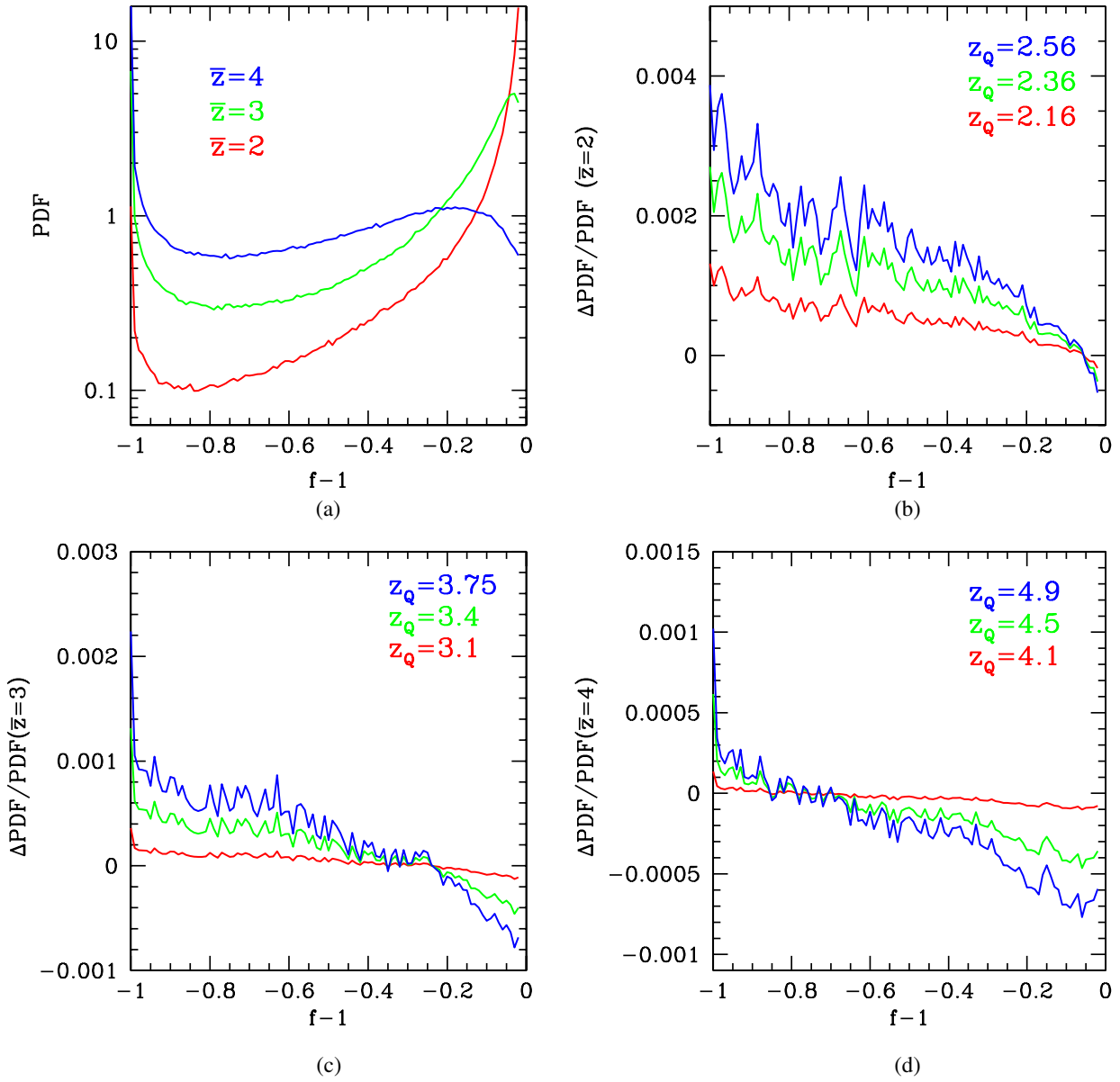

FIG. 4 (color online). (a) The flux probability distribution as measured from the simulations. Panels (b)–(d) show the fractional correction from magnification for mean redshifts $\bar{z} = 2, 3, 4$. The amplitude of the correction depends on the redshift of the quasar z_Q and the slope of the quasar number count function, here we assume $5s - 2 = 3$ [Eq. (6)].

of this one-point statistic is thus related to a two-point correlation, just as the lensing bias of the power spectrum is determined by the bispectrum. As before, to evaluate the bias using this method, an extrapolation of the simulation P_{fm} to $k_\parallel = 0$ is necessary (see Appendix B). We find results that are consistent with those obtained by the weighting method (Fig. 3) to about 30%, with the latter generally higher.

E. Bias to the flux probability distribution function

Another interesting statistic of the Lyman-α forest is the flux PDF: $\mathcal{P}(f)df$ describes the probability that the observed flux lies between $f - df/2$ and $f + df/2$. Here f is the continuum-normalized flux (i.e. f/f_c from the previous section).

The flux PDF measured from simulations with bins of $df = 0.01$ is shown in panel (a) of Fig. 4.[5] The fractional correction from lensing magnification is shown in panels (b)–(d) of the same figure. The effect of magnification is to boost the low flux (high absorption) end of the

[5]We use the same fake continuum fitting procedure described in footnote 4, but again this appears to make little difference to the size of the fractional lensing correction.

PDF and decrease the PDF at the high flux end. The correction is $<1\%$, so unimportant at the current level of precision (5–10% on the flux PDF in bins of $df = 0.05$ [31] but see also [32–34]).

It has been suggested that to avoid systematic errors from continuum fitting one should measure the PDF for fluctuations in the flux $\delta_f = f/\bar{f} - 1$ rather than measuring the PDF of f [35]. In this case the flux is normalized along each line of sight, so the range of δ_f for one line of sight is -1 to $1/\bar{f} - 1$ where $\bar{f}$ is the mean flux along that line of sight. The range of the entire PDF determined from many lines of sight will be -1 to $1/\bar{f}_{\rm min} - 1$, where $\bar{f}_{\rm min}$ is the mean flux along the line of sight with the lowest transmission.

The PDF for δ_f is shown in panel (a) of Fig. 5. Again the fractional correction due to lensing is shown in panels (b)–(d). In this case the correction due to lensing appears rather large at high δ_f. The high δ_f bins are dominated by lines of sight with the lowest mean flux, which are also most highly magnified. However, these high δ_f pixels are quite rare, i.e. the PDF at high δ_f is quite small and therefore noisy from an observational point of view.

For an analytical estimate we apply the fundamental Eq. (8),

$$\langle \mathcal{P}(f)_{\rm obs} \rangle - \mathcal{P}(f)_{\rm true} = \langle \mathcal{P}(f)\delta^{\mu} \rangle, \tag{17}$$

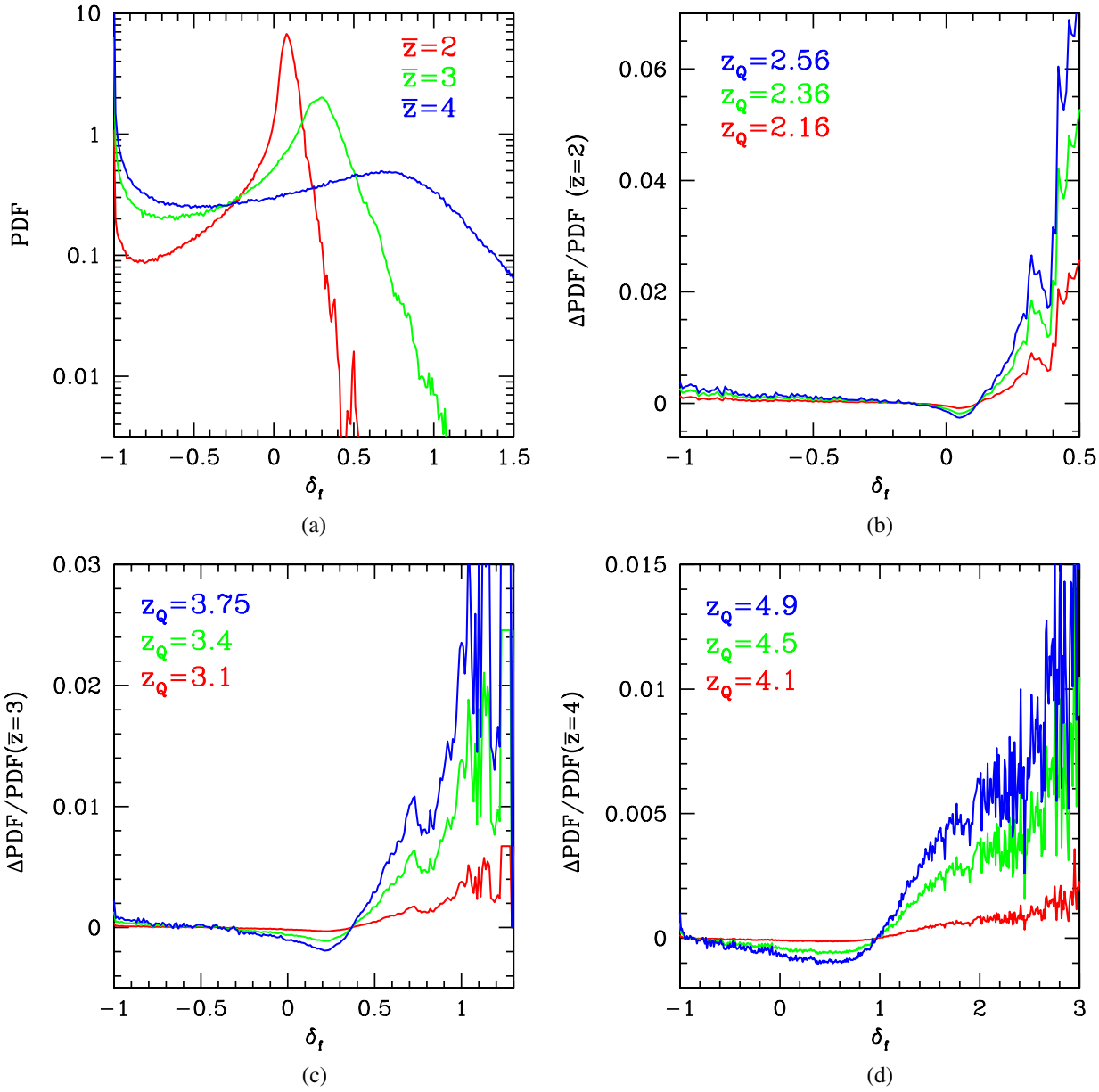

FIG. 5 (color online). (a) The probability distribution function for δ_f as measured from the simulations. Panels (b)–(d) show the fractional correction from magnification for mean redshifts $\bar{z} = 2, 3, 4$.

where $\mathcal{P}(f)df$ is estimated from each line of sight in the standard fashion: counting the fraction of pixels with a flux that falls within df of f. The flux is a nonlinear function of the gas density, but for simplicity, we will assume that gas traces mass and that f is a local function of the mass fluctuation δ, i.e. $f = F(\delta)$, where the function F is to be specified. Let us use the symbol p to denote the (average) location of interest, i.e. δ_p is the mass fluctuation at point p. Thus, the flux PDF at p can be expressed in terms of the mass PDF $\mathcal{P}_m(\delta_p)$:

$$\mathcal{P}(f) = \int d\delta_p \mathcal{P}_m(\delta_p)\delta_D(f - F(\delta_p)) = \int d\delta_p d\delta_l \mathcal{P}_m(\delta_p, \delta_l)\delta_D(f - F(\delta_p)), \quad (18)$$

where δ_D is the Dirac delta function. For the second equality, we have introduced δ_l which is the mass fluctuation at some other point (the subscript l is used in anticipation of the fact that this will be where some lens is), and $\mathcal{P}_m(\delta_p, \delta_l)$ is the joint mass PDF at the two points, i.e. the one-point PDF $\mathcal{P}_m(\delta_p)$ is related to the two-point PDF by $\mathcal{P}_m(\delta_p) = \int d\delta_l \mathcal{P}_m(\delta_p, \delta_l)$. The motivation for introducing the two-point mass PDF is to ease the computation of $\langle \mathcal{P}(f)\delta^\mu \rangle$, where δ^μ involves a line-of-sight integral over locations that generally differ from p. We obtain:[6]

$$\langle \mathcal{P}(f)\delta^\mu \rangle = \frac{3}{2}H_0^2\Omega_m(5s-2)\int_0^{\chi_Q} d\chi_l \frac{\chi_Q - \chi_l}{\chi_Q}\chi_l(1+z_l) \times \int d\delta_p d\delta_l \delta_l \mathcal{P}_m(\delta_p, \delta_l)\delta_D(f - F(\delta_p)). \quad (19)$$

We need a model for the two-point mass PDF. In linear theory, that is completely specified by the two-point correlation $\langle \delta_p \delta_l \rangle$. The relevant fluctuations in the forest are not quite linear. Instead, we will adopt the log-normal model (see for example [36,37]):

$$\mathcal{P}_m(\delta_p, \delta_l) = \frac{1}{2\pi\sqrt{\det \mathbf{C}}(1+\delta_p)(1+\delta_l)} e^{-(1/2)\mathbf{\Delta}^T \mathbf{C}^{-1}\mathbf{\Delta}}, \quad (20)$$

where $\mathbf{\Delta}$ is a 2-component vector with $\Delta_i = \ln(1+\delta_i) + \frac{1}{2}\ln(1+\langle\delta_i^2\rangle)$, and $\mathbf{C}$ is a 2×2 matrix with components $C_{ij} = \ln(1+\langle\delta_i\delta_j\rangle)$. Here i and j stand for p or l. The log-normal model is simply one in which Δ is a Gaussian random field, and the observed δ is related to it by $1+\delta = \exp[\Delta - \langle\Delta^2\rangle/2]$, such that $\langle\Delta^2\rangle = \ln(1+\langle\delta^2\rangle)$. Substituting Eq. (20) into Eq. (19) and integrating over δ_p and δ_l, we find

$$\frac{\langle \mathcal{P}(f)_{\rm obs}\rangle - \mathcal{P}(f)_{\rm true}}{\mathcal{P}(f)_{\rm true}} = \frac{3}{2}\Omega_m(5s-2)H_0^2\int_0^{\chi_Q} d\chi_l \frac{\chi_Q - \chi_l}{\chi_Q}\chi_l(1+z_l) \times (e^{C_{lp}/C_{pp}\ln(1+\delta_*)+(1/2)(C_{lp}-C_{lp}^2/C_{pp}))} - 1), \quad (21)$$

where $\delta_* \equiv F^{-1}(f)$ is the actual density such that the observed flux equals the value of interest f. At this point, we need to specify F: We use $F(\delta) = \exp[-A(1+\delta)^\beta]$, with $\beta = 1.58$ and $A = 0.2010$, 0.9578, 2.960 at $z_p = 2$, 3, 4, respectively. This approximates well what is in our simulations, though the simulated spectra were computed using the exact relation between the optical depth, baryon density, temperature, and ionizing background.

To use Eq. (21), we need C_{lp} and C_{pp}, which we compute using the nonlinear mass power spectrum, with suitable smoothing (for p) to account for the effective Jeans smoothing of baryons. The cosmology and power spectrum prescriptions are described at the end of Sec. II A. Figure 6 compares the analytic calculation in Eq. (21) with the results from simulations in Sec. II B. The two methods agree remarkably well considering the simplicity of the analytic method. If the linear mass PDF were used, the calculated correction has a slightly different f dependence and is typically smaller by about a factor of 5–6.

We should mention data that do not resolve the Jeans scale (or roughly, the thermal broadening scale) have an additional complication: even if the fundamental mass density is log normal distributed (in both one-point and

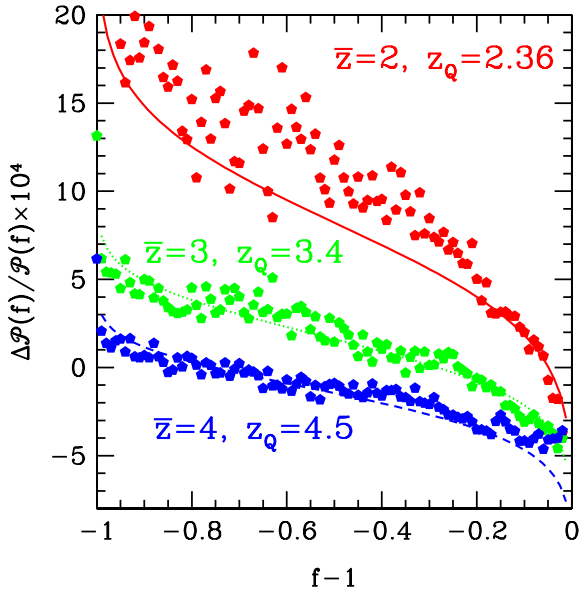

FIG. 6 (color online). The correction to the flux PDF from the analytic model described in Eq. (21) [solid lines] compared with the results from simulations (points). The analytic description with the log-normal model for the mass PDF works surprisingly well.

[6]Here, we are abusing the notation a bit. On the left, $\mathcal{P}(f)$ strictly speaking denotes a stochastic quantity: it should be the estimator that simply counts the fraction of relevant pixels, whereas on the right, $\mathcal{P}_m(\delta, \delta')$ denotes the true (nonstochastic) two-point mass PDF.

two-point sense), the flux field smoothed with a coarse resolution might not be well described by our model. In other words, smoothing and nonlinear transformation do not commute. In any case, the lensing effect on the flux PDF appears to be fairly small.

III. LENSING AS SIGNAL: A TEST OF HOW NEUTRAL HYDROGEN TRACES MASS

In the previous section, we have been exploring lensing as a source of measurement bias. Here, we explore the converse: lensing as a useful signal. We are interested in ways to extract signals of gravitational lensing from Lyman-α forest observations and thereby constrain the cross correlations between flux and mass [for example, the flux-mass power spectrum and flux-flux-mass bispectrum present in Eqs. (14) and (16)].

One option is to correlate the magnitude of quasars with Lyman-α forest observables (we will consider other possible cross correlations at the end of this section). Given some observable $\mathcal{O}_I$ measured from a quasar labeled I, and its magnitude m_I, we can form an estimator $\mathcal{E}$:

$$\mathcal{E} = \frac{1}{N_{\rm QSO}}\sum_I m_I\mathcal{O}_I - \frac{1}{N_{\rm QSO}^2}\Big(\sum_I m_I\Big)\Big(\sum_I \mathcal{O}_I\Big), \tag{22}$$

where $N_{\rm QSO}$ is the number of quasars in one's sample. As is explained in Sec. II A, the Lyman-α forest observable is always implicitly weighted by the number density of quasars (determined by the sample selection). And the quasar magnitude is of course modified by lensing, following from Eq. (1):

$$\delta m = -5\kappa/\ln 10. \tag{23}$$

It is shown in Appendix A that

$$\langle\mathcal{E}\rangle = 5\tilde{s}\langle\kappa\delta\mathcal{O}\rangle, \tag{24}$$

where $\delta\mathcal{O}$ represents fluctuations in $\mathcal{O}$ and $\tilde{s}$ is defined as

$$\tilde{s} \equiv \frac{1}{\ln 10}\frac{\int dm\epsilon(m)(dn^0/dm)(m-\bar{m})}{\int dm\epsilon(m)n^0(m)}, \tag{25}$$

where $\bar{m}$ is the average magnitude in the sample i.e. $\bar{m} = \int dmm\epsilon(m)n^0(m)/\int dm\epsilon(m)n^0(m)$, and $n^0(m)$ and $\epsilon(m)$ are the luminosity function and selection function, respectively—the definition for $\tilde{s}$ is chosen to resemble those for s and s' [Eqs. (2) and (10)]. The $\tilde{s}$ defined here is related to C_S defined in [6] by $C_S = -\ln 10\tilde{s}$. As first emphasized by [6], $C_S = 0$ for a strictly power-law luminosity function in the sense of $n^0(m) \propto e^m$. The realistic quasar luminosity function is not of this form, and we will adopt $C_S \sim 1/3$ from [6], or equivalently $\tilde{s} \sim -0.14$, for our numerical estimates below. The normalizing factor in Eq. (24) is therefore $5\tilde{s} \sim -0.7$. It is worth emphasizing that there is no "-2" term here, unlike for instance $5s - 2$ in Eq. (8). The -2 there arises from the geometrical increase in area by magnification. The statistic $\mathcal{E}$ under consideration is immune to this effect. Further discussions can be found in Appendix A.

A. Magnitude-flux correlation

Let us first consider cross correlations between $\mathcal{O} = \delta_f$, the intervening flux fluctuation, and the quasar magnitude m, giving

$$\langle\mathcal{E}_{\delta m\delta_f}(\chi_Q,\chi)\rangle = 5\tilde{s}\langle\kappa\delta_f\rangle \approx \frac{3}{2}H_0^2\Omega_m 5\tilde{s}\frac{\chi_Q-\chi}{\chi_Q}\chi(1+z)P_{fm}(k_\parallel=0), \tag{26}$$

where χ_Q is the distance to quasar, χ is the distance to absorption (i.e. where δ_f is located) and z is the corresponding redshift. Here, P_{fm} is the (true) 1D flux-mass power spectrum—the subscript m of P_{fm} stands for mass rather than magnitude (just as in Sec. II D).

The nice thing about the estimator $\mathcal{E}_{\delta m\delta_f}$ is that it is expected to depend on the location of absorption χ in a predictable way, which allows this to be separated from other possible systematic effects, an example of which is large-scale power from the uncertain continuum (shape). The fact that the amplitude of this cross correlation signal scales with $\tilde{s}$ can also be exploited to test for consistency, for instance by isolating different subsamples of quasars with different values of $\tilde{s}$.

In Fig. 7 we show the expected signal for this cross correlation as a function of distance to the quasar $\chi_Q - \chi$, where χ is the distance to the absorption. To estimate the overall statistical significance, we can combine the measurements at different separations into an estimate for a single amplitude, namely $P_{fm}(k_\parallel = 0)$. The appropriate minimum variance estimator is described in Appendix C, where we also derive its signal to noise:

$$\frac{S}{N} = \sqrt{\frac{N_{\rm QSO}}{\langle\delta m^2\rangle}\int\frac{dk_\parallel}{2\pi}\frac{|\mathcal{E}_{\delta m\delta_f}(k_\parallel)|^2}{P_{ff}(k_\parallel)+\mathcal{S}.\mathcal{N}.}}, \tag{27}$$

where $\mathcal{E}_{\delta m\delta_f}(k_\parallel)$ is the Fourier transform (over χ) of Eq. (26), $N_{\rm QSO}$ is the number of quasars available, $\langle\delta m^2\rangle$ is the quasar magnitude variance, P_{ff} is the 1D flux-power spectrum, and $\mathcal{S}.\mathcal{N}.$ is the associated shot-noise.

The $\mathcal{S}.\mathcal{N}.$ term is important so we consider the signal to noise per quasar for two survey configurations: "SDSS III configuration" with resolution FWHM is 60 km/s, and the shot-noise power is $\sim$0.44 Mpc/h $(3/(1+\bar{z}))^{3/2}$ [38] and "Keck configuration" with resolution FWHM is 10 km/s and shot-noise power is $\sim$0.029 Mpc/h $(3/(1+\bar{z}))^{3/2}$. For both we take the magnitude dispersion of the quasar sample to be 0.5 [6]. The first set of numbers roughly resemble the expectations of SDSS III [39] but keep in mind the configuration we assume likely differs a bit from

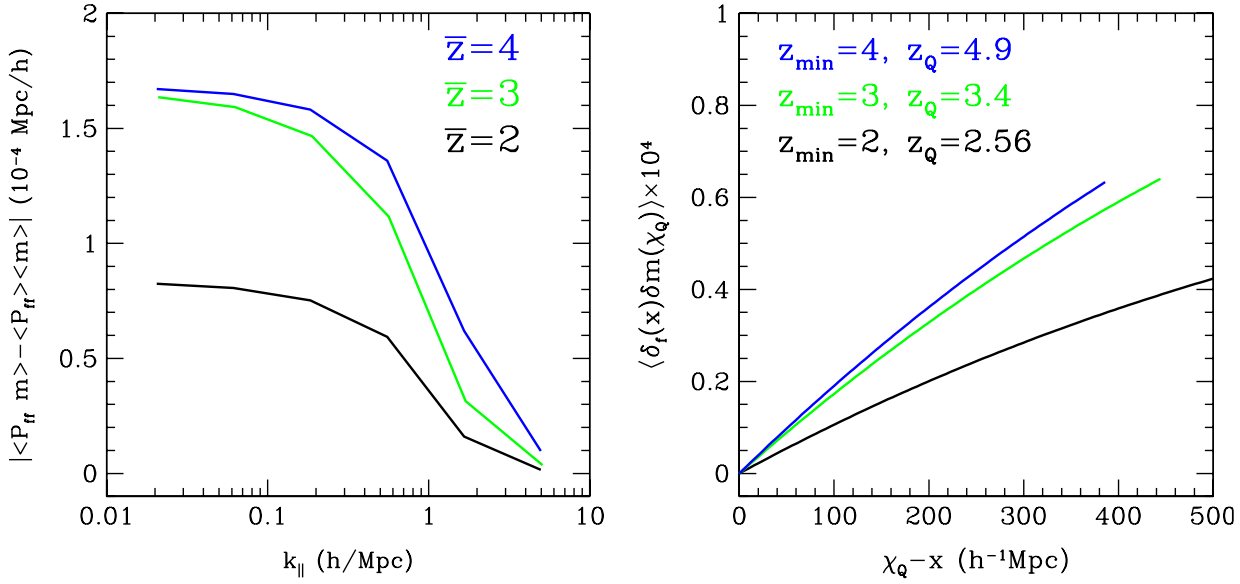

FIG. 7 (color online). Left: The lensing-induced correlation between quasar magnitude and the flux-power spectrum given in Eq. (28). The amplitude of the signal increases with increasing distance between $\chi(\bar{z})$ and the background quasar but above we assume the correlation is averaged over background quasars at redshifts between $\bar{z}+0.1$ and $z_\beta=\nu_\beta/\nu_\alpha(1+\bar{z})-1$ (the maximum redshift for the quasar before confusion between Lyman-α and Lyman-β absorption sets in). Right: The magnitude-flux cross correlation [Eq. (26)] as a function of line of sight comoving distance to the quasar.

what will turn out in practice. The results for the S/N per sight line are summarized in Table I. For the SDSS III expectation of $N_Q=160\,000$ the S/N for this amplitude is expected to be only $\sim$1 and even for a futuristic survey like BigBOSS [40] that could measure 10^6 spectra with similar resolution only $S/N\sim2$–3 could be achieved. Comparison with the "Keck configuration" shows that shot noise is clearly a limitation for these observables. However, the S/N estimates presented are for a single redshift bin of width $\Delta z\sim0.2$, but measurements will be made at a range of redshifts which could be combined to get a slightly higher signal-to-noise estimate of, for example, the mean P_{fm} across the redshift span of the survey.

It is worth noting a few points that reduce S/N of the forest-magnitude correlations in comparison with galaxy-magnitude correlations used [6]. (1) The cross correlation between flux and mass is lower than the correlation between galaxies and mass (the correlation coefficient is $\sim P_{fm}/\sqrt{P_{ff}P_{mm}}\lesssim0.5$). (2) Lensing peaks at a distance halfway between the observer and the quasar, but to avoid confusion with Lyman-β we use only the part of the Lyman-α forest near to the quasar where the lensing is smaller. (3) The signal to noise of magnitude-forest correlations is $\propto\sqrt{N_Q}$ where N_Q is the number of quasars with spectra, while for the galaxy-magnitude cross correlation it is proportional to the number of galaxy-quasar pairs $\propto\sqrt{N_Q N_g}$ (however, in Sec. III D we briefly discuss correlating the forest with quasars along different lines of sight).

B. Magnitude-power correlation

Another possibility is to set $\mathcal{O}=P_{ff}(k_\parallel)$ in the estimator Eq. (22), i.e. cross correlate quasar magnitude and the flux-power spectrum. This estimator has the following expectation value:

$$\langle\mathcal{E}_{\delta mP_{ff}}(k_\parallel)\rangle=\frac{5\tilde{s}}{\Delta\chi}\langle\kappa\delta_f(k_\parallel)\delta_f^*(k_\parallel)\rangle, \tag{28}$$

TABLE I. The signal to noise per line-of-sight (l.o.s.) in redshift bins of $\Delta z\sim0.2$ for the proposed estimators in Eqs. (26), (29), and (30) for the SDSS III and Keck survey configurations (see Sec. III A). Here, we assume the quasar sample has $\tilde{s}=-0.14$ [see Eq. (25)] and the quasar magnitude dispersion is 0.5. For $\langle f/f_C\delta m\rangle$ we assume the same fractional errors of f/f_C as [30] and that the errors are statistics limited so they scale as $1/\sqrt{N_{\rm QSO}}$.

Observable:	S/N per l.o.s. for SDSS III configuration	S/N per l.o.s. for Keck configuration
$\langle\delta_f\delta m\rangle$ at $z=2,3,4$	0.002, 0.0029, 0.0022	0.0041, 0.0036, 0.0024
$\langle\delta P_{ff}\delta m\rangle$ at $z=2,3,4$	0.0016, 0.0028, 0.0025	0.008, 0.006, 0.0042
$\langle f/f_C\delta m\rangle$ at $z=2,3,4$	0.0054, 0.0032, 0.000 95	-

where $\Delta\chi$ is the length of the quasar spectra from which the power is measured. This expression is similar to Eq. (13), and indeed one can relate this to the bias in P_{ff} measurement we have calculated in Sec. II C [Eq. (14)]:

$$\langle \mathcal{E}_{\delta m P_{ff}}(k_\parallel)\rangle = \frac{5\tilde{s}}{5s-2}(\langle P_{ff\,\mathrm{obs}}(k_\parallel)\rangle - P_{ff\,\mathrm{true}}(k_\parallel)). \quad (29)$$

This means that one could in principle use the magnitude-power correlation to correct for the bias in P_{ff} measurement. The expected magnitude-power correlation is shown in Fig. 7 and the signal to noise is given in Table I.

C. Magnitude-mean-transmission correlation

If the continuum can be accurately estimated, one could also correlate the mean transmission from each line of sight with the quasar magnitude behind it, i.e. choose $\mathcal{O} = [f/f_C]$ where f is the observed flux and f_C is the continuum, and the brackets [] denote an average along the line of sight. One can see that the expected correlation should be related to the bias in $e^{-\tau_{\mathrm{eff}}}$ discussed in Sec. IV:

$$\langle \mathcal{E}_{\delta m[f/f_C]}\rangle = \frac{5\tilde{s}}{5s-2}(\langle e^{-\tau_{\mathrm{eff}}}{}_{\mathrm{obs}}\rangle - e^{-\tau_{\mathrm{eff}}}{}_{\mathrm{true}}). \quad (30)$$

The signal to noise per sight line is listed in Table I. Note that the number of quasars needed is realistic only if the continuum is estimated by extrapolating from the red side (such as in the analysis of [30]). The number of quasars should be much smaller if the continuum were estimated by performing a smooth fit through portions of the Lyman-α forest that are deemed unabsorbed, a method that typically requires high resolution data. Whichever the continuum estimation method, care should be taken in accounting for possible systematic biases (in the continuum estimate) when interpreting this cross correlation measurement.

D. Additional cross correlations

We have focused on cross correlations between the quasar magnitude and a Lyman-α forest observable *in the same line of sight*. There are two possible extensions we should mention in passing. One is that the quasar magnitude and the Lyman-α forest observable can come from *different lines of sight*. In other words, the cross correlations can be measured at a nonzero angular separation. On the one hand, the forest-magnitude correlation should drop off rapidly with increasing angular separation decreasing the signal, however the noise is reduced by the number of quasar pairs at a given angular separation. Roughly, the signal to noise for lines of sight at angular separation θ should scale as

$$\left(\frac{S}{N}\right)_{\mathrm{at\ sep.}\theta} \sim \left(\frac{S}{N}\right)_{\mathrm{same\ l.o.s.}} \frac{10(\chi_Q - \bar{\chi})}{\chi_Q} \frac{w_{fm}(\theta)}{w_{fm}(\theta=0)} \times \sqrt{\frac{N_{\mathrm{pairs}}(\theta)}{N_Q}}, \quad (31)$$

where $w_{fm}(\theta)$ is the angular flux-mass correlation function, $N_{\mathrm{pairs}}(\theta)$ is the number of quasar pairs with angular separation θ and the term with the ratio of the distances roughly accounts for the fact that this correlation does not require $\bar{z}$ to be above the Lyman-β confusion limit for the quasar (previously we needed $\bar{\chi} > \chi_\beta \sim 4/5\chi_Q$ and had set $\bar{\chi} \sim \chi_\beta + (\chi_Q - \chi_\beta)/2$). It seems that the sparseness of quasars ($\sim 16/(\mathrm{deg})^2$ for SDSS III) does not permit $N_{\mathrm{pairs}}(\theta)$ to be large enough that adding off-axis correlations will drastically improve the signal to noise in the near term.

Another possibility is to cross correlate the quasar number density (which is affected by lensing through magnification bias) with the Lyman-α forest observable. Such a correlation makes sense only at a nonzero lag (or nonzero smoothing), since the Lyman-α forest is observable only if there is a quasar directly behind it. While we do not give explicit estimates here of the signal to noise for these cross correlations, they should be useful in disentangling the lensing signal from certain systematic effects, as we will discuss next.

E. Dust and other systematic effects

We discuss here three systematic effects that could complicate the measurement of the various cross correlations mentioned above.

The first is the continuum. The continuum presumably is smooth and therefore has fluctuations only on large scales. But since its precise shape is uncertain, a cross correlation such as the magnitude-flux correlation is susceptible to possible contamination from continuum power. A fortunate feature of the cross correlation is that it has a definite shape predicted by lensing, as well as an amplitude that scales with $\tilde{s}$. Both can be exploited to check for such a contamination.

The second systematic effect we loosely refer to as "background subtraction." Realistic spectra of quasars inevitably contain "background" which can come from several sources, including the sky and scattered light within the optical instrument. While attempts are generally made to subtract these backgrounds as accurately as possible, there are inevitably residuals. These residuals could correlate with the quasar magnitude, for instance they could be more noticeable for fainter quasars. This would then produce spurious correlations when we correlate the quasar magnitude with Lyman-α forest observables (deduced from imperfect data that contain residual backgrounds). In fact, existing flux-power spectrum measurements from SDSS [27] are known to exhibit an otherwise puzzling correlation: that P_{ff} is systematically higher for fainter

quasars, and this correlation is statistically significant (the normalized correlation coefficient is ~5–10% [41]). Such a correlation can be explained by this background subtraction effect. It cannot be explained by lensing since it tends to produce a correlation of an opposite sign unless $\tilde{s}$ has a sign opposite to what is known. (It can also be plausibly produced by dust which we will discuss below). To disentangle background subtraction issues from lensing, it would be useful to examine magnitude-observable cross correlations at nonzero lag—it would be quite surprising if background residuals cause correlations between quasar magnitude at one point with Lyman-α forest power at another.

The third systematic effect is dust extinction. Dust modifies flux by $f \rightarrow f e^{-\tau_{\rm dust}}$, where $\tau_{\rm dust}$ is the optical depth due to dust. This modification is frequency dependent (higher optical depth for bluer photons), but the frequency (which translates into scale) dependence is mild on the scales of interest, and therefore effectively acts as a continuum. The net magnification plus dust correction to the quasar number density is

$$n \rightarrow n \mu^{2.5s-1} e^{-2.5 s \tau_{\rm dust}}. \quad (32)$$

Including dust extinction, the measurement bias associated with a Lyman-α forest observable [Eq. (8)] is changed to

$$\langle \mathcal{O}_{\rm obs} \rangle - \mathcal{O}_{\rm true} = (5s-2)\langle \mathcal{O}\kappa \rangle - 2.5 s \langle \mathcal{O}\delta\tau_{\rm dust} \rangle, \quad (33)$$

where $\delta\tau_{\rm dust} = \tau_{\rm dust} - \langle \tau_{\rm dust} \rangle$, which is assumed to be small, and we have ignored $\langle \mathcal{O}\kappa\delta\tau_{\rm dust} \rangle$.

As far as the "signal" part of our discussion is concerned, the magnitude-observable cross correlation [Eq. (24)] is modified to

$$\langle \mathcal{E} \rangle = 5\tilde{s}\langle \kappa\delta\mathcal{O} \rangle - 2.5\tilde{s}\langle \delta\tau_{\rm dust}\delta\mathcal{O} \rangle. \quad (34)$$

A full calculation of the effect of dust is beyond the scope of this paper. But given a model for $\delta\tau_{\rm dust}$ the effect can be calculated in a way very similar to lensing—$\tau_{\rm dust}$ after all is another line of sight integral over the (dust) density. Calculations comparing the amplitudes of magnification and dust corrections to supernova flux have shown $\langle \kappa\delta\tau_{\rm dust} \rangle - \langle \delta\tau_{\rm dust}\delta\tau_{\rm dust} \rangle$ to be ~7–40% of $\langle \kappa\kappa \rangle$ at $z_{\rm source} = 1.5$ depending on the dust model [42]. At higher redshifts the dust term is expected to be less important, while the lensing effect should grow. On the other hand, recent measurements suggest that at $z = 0.3$ dust extinction can cause shifts in source magnitude comparable to those caused by lensing magnification [6]. For the Lyman-α forest, which is typically measured at redshifts $z \gtrsim 2$, the dust corrections are likely to be smaller than the lensing corrections but should be included in a full analysis.

IV. DISCUSSION

We have discussed the sampling bias introduced by magnification and dust on measurements of the Lyman-α forest. In calculating the effect of this bias [summarized in Eq. (8)] we made the assumption that all quasar spectra are weighted equally. If, on the other hand, forest measurements were weighted by quasar flux, the effect of lensing bias would be larger than what we have found [see, for example, Eq. (9)].

If the quasars are weighted uniformly, we find that magnification bias leads to corrections $\lesssim 1\%$ to the flux-power spectrum (Fig. 1), $\lesssim 0.1\%$ to the effective optical depth (Fig. 2), $\lesssim 0.1\%$ to the flux probability distribution function $\mathcal{P}(f)$, and as large as a few % to the probability distribution function for the flux fluctuation $\mathcal{P}(\delta_f)$ (see Figs. 4 and 5). These estimates assume quasar number count slope $s = 1$, probably reasonable for the SDSS quasars used for Lyman-α forest measurements. The lensing correction varies strongly with redshift with larger corrections present at lower redshift, largely due to nonlinear growth of mass fluctuations. The biases induced by magnification to the effective optical depth are significantly smaller than current error bars. For the flux-power spectrum, the lensing bias is just within the current error bars, and since it leads to a systematic offset in each data point, may effect measurements of the overall amplitude of the power spectrum. At low redshift the lensing effect on the PDF of δ_f can be rather large, reaching several percent at the high δ_f end of the PDF at $z = 2$, however this occurs only in regions where the PDF itself is very small $\lesssim 0.1$. Lensing magnification is probably unimportant for current measurements of the flux PDF and the quantities derived from it.

One may wonder whether including nonlinear magnification[7]—which is more important at the small angular separations relevant for the Lyman-α forest—could change our results. We have checked that including all κ terms contributing to μ in Eqs. (2) and (11), rather than just the linear term as in Eq. (6), changes the magnification bias corrections by $\lesssim 2\%$. The true nonlinear magnification of course depends on the components of the shear as well as the lensing convergence but it would be surprising if they drastically changed our (all orders in κ) estimate of their importance.[8]

[7]To be precise, the true magnification $\mu = 1/((1-\kappa)^2 - \gamma_1^2 - \gamma_2^2)$ where γ_1 and γ_2 are the shear. Throughout this paper we assume κ, γ_1, γ_2 are small quantities and so we keep only the first order terms in the expression for μ. Nonlinear magnification refers to the higher-order (in γ and κ) terms contributing to μ [43].

[8]Actually, there is a further caveat here in that we did not compute the true lensing convergence κ because we have ignored contributions from mass fluctuations at the lower redshifts outside the box. For the nonlinear terms, this should not be a good approximation (e.g. $\langle \kappa\kappa \rangle$ is poorly estimated) nevertheless it would be surprising if this made an orders-of-magnitude difference in the effect of magnification bias. But perhaps this plus the ignored γ terms could increase the importance of nonlinear magnification to the ~20% reported by [43].

An additional caveat to our analysis is that the damped Lyman-α (DLA) systems and their associated damping wings are not accurately modeled by the simulations and mock spectra. While DLAs are rare, magnification bias could make them more abundant in survey samples. The damping wings of DLAs are known to add spurious power to $P_{ff}(k_{||})$ at the 10–20% level on large scales [44]. Magnification bias should increase the abundance of DLAs making the power spectrum more biased than our results suggest. Precisely how magnification affects the DLA bias deserves further investigation.

Perhaps most interesting is that lensing magnification induces a correlation between Lyman-α observables and the magnitude of the quasars used to measure them (Fig. 7). Unfortunately even with the large number of quasar spectra the BOSS survey will obtain it will be a challenge to detect correlations between the flux-power spectrum, the flux decrement or the mean transmission and quasar magnitude with high signal to noise (see Table I). Additionally, it is possible that lines of sight with high magnification also have more metal lines which could further complicate the analysis. Nevertheless these correlations provide a direct measure of how fluctuations in the quasar flux trace the underlying density field, for example, they could *directly* constrain the flux-mass power spectrum and should therefore be targeted. A more thorough analysis of how to detect the flux-magnitude and flux-power correlations is necessary, we leave this to future work. For a recent idea in a similar vein see [13,14] who propose correlating lensing in the cosmic microwave background with fluctuations in the forest to extract flux-mass information.

It is worth noting that, with a large quasar sample, it may be possible to exploit the dependence on $5s - 2$ and/or $\chi(z_Q)$ to isolate the magnification correction and to measure the flux-magnitude correlations. The lensing correction depends linearly on $5s - 2$, which ranges quite a bit depending on magnitude limit (Fig. 8). In the weak lensing limit the correction scales as $H_0(\chi(z_Q) - \chi(z))\chi(z)/\chi(z_Q)$ which varies from $\sim \frac{4}{25} H_0 \chi(z_Q)$ to 0 as z goes from z_β and z_Q. Indeed measuring these distinctive dependencies would help guard against possible instrumental systematics from being confused with the lensing signal. Our estimates of the forest-magnitude correlations in Secs. III A, III B, III C, and III D assumed z was halfway between z_β and z_Q. Also, there exist in public data $\sim$150 close quasar pairs [45], that one might wish to use for this analysis, unfortunately their number is small compared to the 10^5 expected from SDSS III and will not significantly improve the signal to noise.

There is quite a bit of interest in using the Lyman-α forest to map the 3D density field and use, for example, the baryon features in the two-point correlation function or power spectrum to constrain dark energy and the expansion history of the universe [46]. While we have focused on the power spectrum gotten from 1D measurements of the flux

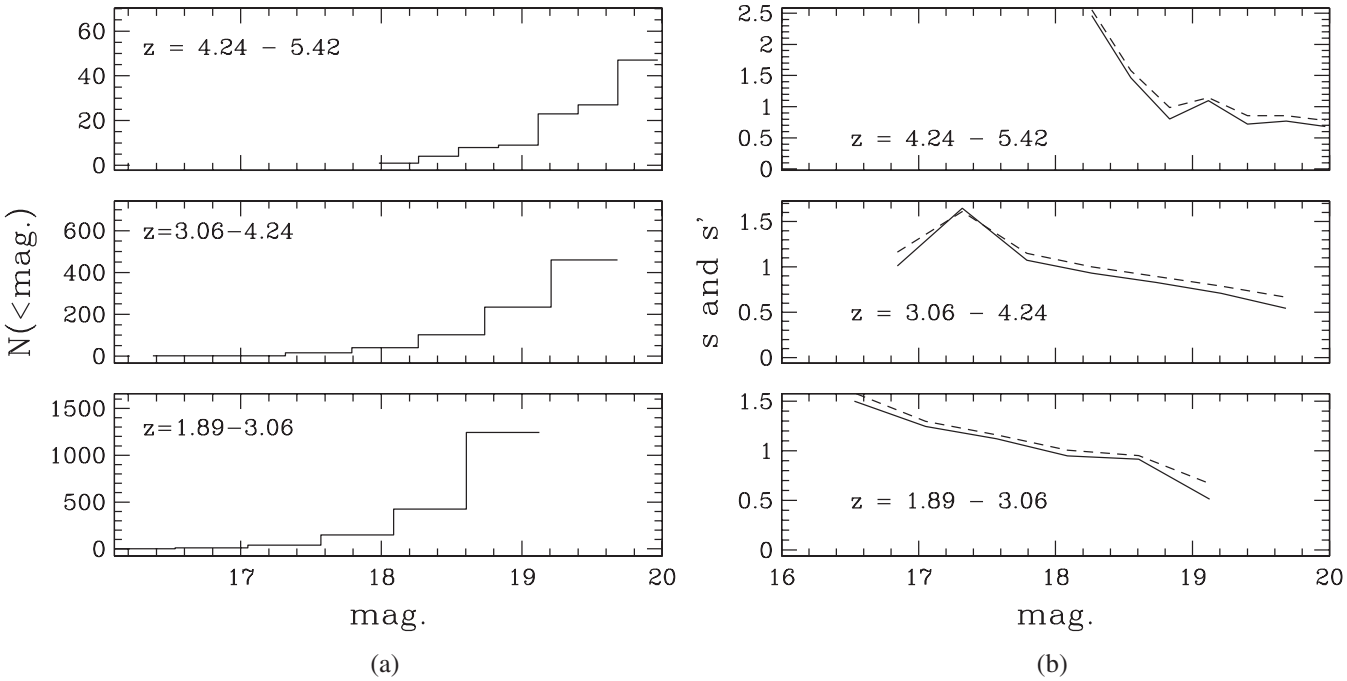

FIG. 8. (a) A histogram of the number of quasars as function of i-band magnitude measured from the Sloan Digital Sky Survey. (b) The slopes s (solid) and s' (dashed) defined in Eqs. (2) and (10) as a function of the limiting magnitude (i.e. assuming a step function ϵ). These measurements ignore possible incompleteness in the data, and are therefore likely underestimates, especially at the faint end.

fluctuation, the analysis could be extended to include correlations between different quasar spectra (and therefore different sight lines). Additional corrections due to correlations between flux and convergence across different lines of sight ($\sim\langle\delta_f(\chi\boldsymbol{\theta})\delta_f(\chi'\boldsymbol{\theta}')\kappa(\chi\boldsymbol{\theta})\rangle$) would arise. However, since lensing is strongest for lenses along the same line of sight as the sources, the terms calculated in this work should be dominant. One would therefore expect the lensing bias to the correlation function around the baryon scale to remain 0.1–1%.[9]

ACKNOWLEDGMENTS

We are extremely grateful to L. Hernquist and V. Springel for providing us with the simulations data used in our analyses. We thank D. Hogg, G. Kauffman, I. McGreer, U. Seljak, D. Spergel, and D. Weinberg for discussions. L. H. thanks members of the CCPP (New York), CITA (Toronto), and IAS (Princeton) for their fabulous hospitality. M. L. and L. H. acknowledge support from the DOE under Contract No. DE-FG02-92ER40699, the NASA ATP under Contract No. 09-ATP09-0049, and the Initiatives in Science and Engineering Program at Columbia University. S. M. is supported by the Cyprus State Foundation. M. L. is supported as a Friends of the Institute for Advanced Study Member.

APPENDIX A: DERIVATION OF MAGNITUDE, NUMBER AND OBSERVABLE CROSS CORRELATIONS

In this appendix, we derive the main results of this paper in a unified manner. They include the lensing-induced measurement bias (for both uniform and flux weighting) and the general magnitude-observable cross correlation, described, respectively, in Eqs. (2), (8), (9), and (24). Most of these reduce to known results in the literature for a step-function selection.

All quantities of interest take the following form:

$$Q = \frac{\sum_I w_I \mathcal{O}_I}{\sum_I u_I}, \tag{A1}$$

where I sums over quasars in one's sample, w_I and u_I are explicit weights one might apply to them (w_I and u_I might or might not be equal), and $\mathcal{O}_I$ is a Lyman-α forest observable associated with quasar I.

It is helpful following Sec. II A to conceptually pixelize the survey (with pixel label i), and rewrite this as

$$Q = \frac{\sum_i \int dm w(m)\epsilon(m)n_i(m)\mathcal{O}_i}{\sum_i \int dm u(m)\epsilon(m)n_i(m)}, \tag{36}$$

where $dmn_i(m)$ is the number density of quasars at pixel i with magnitude $m \pm dm/2$, $\epsilon(m)$ is the selection function (e.g. $\epsilon(m)$ could be 1 for all quasars brighter than some limit $m_{\rm lim}$ and 0 otherwise), and we assume the weights w and u are functions of the observed quasar magnitude m.

Recall that lensing modifies the observe flux by $f \to f + \delta f = f\mu = f(1 + 2\kappa)$, where κ is the (weak) lensing convergence defined previously in Eq. (6). Flux and magnitude are related by $f = \exp[-m\ln 10/2.5]$, and so $m = m^0 + \delta m = m^0 - \frac{5}{\ln 10}\kappa$, where m^0 and m are the unlensed and lensed magnitudes, respectively, [Eq. (23)]. The observed number density of quasars $n_i(m)dm$ is related to the pre-lensed number density $n_i^0(m^0)dm^0$ by

$$n_i(m)dm = n_i^0(m^0)dm^0\frac{1}{1+2\kappa_i}, \tag{A3}$$

where $1/(1 + 2\kappa_i)$ factor accounts for the geometrical increase in area by magnification (and therefore reduction in number density). Taylor expanding gives us

$$n_i(m) = n_i^0(m) + \left(\frac{2.5}{\ln 10}\frac{dn_i^0(m)}{dm} - n_i^0(m)\right)2\kappa_i. \tag{A4}$$

The denominator of Q is well approximated by

$$\text{denominator of } Q = \sum_i \int dm u(m)\epsilon(m)n^0(m), \tag{A5}$$

where we have assumed that the survey is large enough that under the summation over pixels i, $n_i^0(m)$ which could fluctuate from pixel to pixel can be replaced by its average $n^0(m)$ (i.e. the true pre-lensed luminosity function), and $\sum_i \kappa_i \sim 0$. The summation $\sum_i$ then simply gives the number of pixels in the survey. This kind of approximation is equivalent to ignoring corrections of the integral constraint type [15].

The numerator of Q can be computed by rewriting $\mathcal{O}_i = \mathcal{O}_{\rm true} + \delta\mathcal{O}_i$, where $\mathcal{O}_{\rm true}$ denotes the ensemble average $\mathcal{O}_{\rm true} = \langle\mathcal{O}_i\rangle$ (i.e. an average over ensemble of realizations of the universe). Assuming there is neither correlation between $\mathcal{O}_i$ and the pre-lensed number density n_i^0, nor correlation between κ_i and n_i^0, we find

$$\begin{aligned}\langle\text{numerator of } Q\rangle = &\sum_i \int dm w(m)\epsilon(m)n^0(m)\mathcal{O}_{\rm true} \\ &+ \sum_i \int dm w(m)\epsilon(m)\left(\frac{2.5}{\ln 10}\frac{dn^0(m)}{dm}\right. \\ &\left. - n^0(m)\right)2\langle\kappa\delta\mathcal{O}\rangle,\end{aligned} \tag{A6}$$

where we have dropped the i label from $\langle\kappa_i\delta\mathcal{O}_i\rangle$ since this is simply a cross correlation at zero lag. Just as for the denominator, the summation $\sum_i$ reduces simply to the total number of pixels.

[9] We have checked that unlike the case of the 3D galaxy correlation function [47,48] nothing is remarkably different about the lensing bias to the real space flux correlation function as compared to Fourier space.

In summary, we find

$$\langle Q\rangle = \mathcal{O}_{\rm true}\frac{\int dm w(m)\epsilon(m)n^0(m)}{\int dm u(m)\epsilon(m)n^0(m)} + 2\langle\kappa\delta\mathcal{O}\rangle \times \frac{\int dm w(m)\epsilon(m)(\frac{2.5}{\ln 10}\frac{dn^0(m)}{dm} - n^0(m))}{\int dm u(m)\epsilon(m)n^0(m)}. \quad \text{(A7)}$$

This is a fundamental result from which everything follows. Let us first apply it to the case with $w(m) = u(m) = 1$ i.e. Q is what we have been calling $\mathcal{O}_{\rm obs}$, with equal weights applied to all quasars *within* one's sample. Equation (A7) tells us

$$\langle\mathcal{O}_{\rm obs}\rangle = \mathcal{O}_{\rm true} + (5s-2)\langle\kappa\delta\mathcal{O}\rangle, \qquad s = \frac{1}{\ln 10}\frac{\int dm\epsilon(m)(dn^0/dm)}{\int dm\epsilon(m)n^0(m)}, \quad \text{(A8)}$$

consistent with Eq. (8) and the definition of s in Eq. (2). Note that $\langle\kappa\delta\mathcal{O}\rangle = \langle\kappa\mathcal{O}\rangle$ since $\langle\kappa\rangle = 0$. If the selection function $\epsilon(m)$ were a step function, s reduces to the more familiar slope of the quasar number count upon integration by parts (see Sec. I).

Let us next try $w(m) = u(m) = \exp[-m\ln 10/2.5]$ in Eq. (A7), i.e. Q is equivalent to $\mathcal{O}_{\rm obs}$, with a flux weighting. It is simple to see that

$$\langle\mathcal{O}_{\rm obs}\rangle = \mathcal{O}_{\rm true} + (5s'-2)\langle\kappa\delta\mathcal{O}\rangle, \qquad s' = \frac{1}{\ln 10}\frac{\int dm\epsilon(m)(dn^0/dm)10^{-m/2.5}}{\int dm\epsilon(m)n^0(m)10^{-m/2.5}}, \quad \text{(A9)}$$

which is consistent with Eqs. (9) and (10).

Lastly, let us use $w(m) = m - \bar{m}$ and $u(m) = 1$ in Eq. (A7), with $\bar{m} = \int dm m\epsilon(m)n^0(m)/\int dm\epsilon(m)n^0(m)$. Then, Q corresponds to the cross correlation estimator $\mathcal{E}$ of Eq. (22), keeping in mind that $\bar{m}$ (which is the average sample magnitude defined by the *true* unlensed luminosity function) should be well approximated by $\sum_I m_I/\sum_I$ for a sufficiently large survey. We obtain

$$\langle\mathcal{E}\rangle = 5\tilde{s}\langle\kappa\delta\mathcal{O}\rangle, \qquad \tilde{s} \equiv \frac{1}{\ln 10}\frac{\int dm\epsilon(m)(dn^0/dm)(m-\bar{m})}{\int dm\epsilon(m)n^0(m)}, \quad \text{(A10)}$$

which is consistent with Eqs. (24) and (25). Note how the -2 that is present in both Eqs. (A8) and (A9) is absent in (A10). In the first two cases, this -2 originates from the "$-n^0(m)$" in the second term of Eq. (A10). This term yields zero in Eq. (A10) by definition of $w(m) = m - \bar{m}$.

The different symbols s, s' and $\tilde{s}$ can be seen as different (normalized) moments of $\epsilon(m)dn^0/dm$. In Fig. 8 we show the cumulated number counts and rough estimates of s and s' from SDSS data release 6. It is worth emphasizing that incompleteness is not taken into account in deducing these estimates, and the true values of s and s' could well be higher, especially at the faint end. In other words, if incompleteness is present, it should be properly taken into account through the efficiency $\epsilon(m)$. Blindly measuring s by taking derivative of the *observed* (i.e. incomplete) cumulated number count would result in an underestimate.

APPENDIX B: DETERMINING THE LOW-k BISPECTRUM

In this appendix we discuss how we determine the flux-flux-mass bispectrum at low $k_{||}$. The issue is that the simulations have a finite box size, and we need to extrapolate $B_{ffm}(k_{||}, -(k_{||}+k'_{||}), k'_{||})$ from $k'_{||} \sim 2\pi/L$ to $k'_{||} \sim 0$, where L is the size of the box. At $z = 3$ we have simulations in a larger box and we find that doubling the box size (from $L = 50$ Mpc$/h$ to $L = 100$ Mpc$/h$) increases $B_{ffm}(k_{||}, -k_{||}, 0)$ by a factor of about 4. To determine B_{ffm} for very low k we first use a hierarchical model for B_{ffm},

$$B_{ffm}(k_{||}, -(k_{||}+k'_{||}), k'_{||}) = Q_{ffm}(P_{fm}(k_{||})P_{fm}(k'_{||}) + P_{fm}(k_{||})P_{fm}(k_{||}+k'_{||}) + P_{fm}(k'_{||})P_{fm}(k_{||}+k'_{||})). \quad \text{(B1)}$$

This hierarchical model with Q_{ffm} independent of $k_{||}$ but varying with z appears to be a pretty good fit to the simulations-measured bispectrum for $k_{||}$, $k'_{||} \lesssim 1\ h$/Mpc with better agreement $z = 3$ and $z = 4$ than $z = 2$. At $k_{||} \gtrsim 1\ h$/Mpc the hierarchical bispectrum drops off much more rapidly than the true bispectrum. Comparison of the hierarchical and true bispectra is shown in Fig. 9. Given the agreement between the hierarchical and the measured bispectra (on large scales), we now assume Eq. (B1) works at $B_{ffm}(k_{||}, -k_{||}, 0)$ and embark on the somewhat easier task of determining P_{fm} at very low $k_{||}$.

The low $k_{||}$ value of P_{fm} is determined using both the simulations and analytics. Precisely, we set $P_{fm}(k=0) = P^{\rm sims}_{fm}(k_{\rm min})/P^{\rm calc}_{bm}(k_{\rm min}) \times P^{\rm calc}_{bm}(k=0)$. The calculated 1D baryon-mass power spectrum at $k_{||} = 0$ is given by

$$P^{\rm calc}_{bm} = \int \frac{d^2\mathbf{k}_\perp}{(2\pi)^2} P_{3D}(k_\perp) e^{-k_\perp^2/k_s^2}, \quad \text{(B2)}$$

where $P_{3D}(k)$ is the 3D mass power spectrum, $k_s = \sqrt{\frac{10}{3}}k_J$ with $k_J = \sqrt{4\pi G\rho}/(c_s(1+z))$ is the Jeans length for a system with sounds speed c_s [49] and proper mass density ρ. Assuming the intergalactic medium can be treated as a monatomic ideal gas $c_s = \sqrt{5T/(3m)}$ where m is the mean particle mass. For a fully ionized gas composed of 75% Hydrogen and 25% Helium by mass $m = 0.59m_p$ where m_p is the proton mass. We assume $T = 20\,000K$ is the gas temperature constant over the redshift range we are interested in [50].

The reader might wonder whether analytic estimates of the flux-mass power spectrum and flux-flux-mass bispectrum can be used to make accurate predictions without

simulations. A naive guess, $\delta_f = b\delta_b(k)$ works fairly well for P_{fm} but overestimates the magnitude of B_{ffm} by a factor of a few. The dominant reason for this discrepancy appears to be the difference between Q_{ffm} and Q_{mmm}, where Q_{mmm} is the equivalent parameter for the hierarchical mass-mass-mass bispectrum. Hyper-extended perturbation theory [51] suggests that on the scales we are interested in, the hierarchical ansatz should fit the mass bispectrum B_{mmm} with a factor $Q_{mmm} \sim 3$ (and only weakly dependent on redshift). Indeed our simulations give a similar value for Q_{mmm}, and the hierarchical ansatz fits B_{mmm} rather well. However, for the flux-flux-mass bispectrum we find that $Q_{ffm} \lesssim 1$ and varies more strongly with redshift. So, because of this difference the assumption $B_{ffm}(k, k', k'') = b^2 B_{mmm}$ fails even on large-scales where $P_{ff} \sim b^2 P_{mm}$. This is why we have to rely on simulations to obtain an estimate of the flux-flux-mass bispectrum, but making suitable corrections to get at the $(k_\parallel, -k_\parallel, 0)$ limit. It is also worth emphasizing we have estimated the measurement bias associated with the flux-power spectrum two different ways, one using the flux-flux-mass bispectrum and the other does not, and they agree reasonably well (Fig. 2).

APPENDIX C: ESTIMATOR AND ERROR FOR THE MAGNITUDE-FLUX CORRELATION AMPLITUDE

Recall that the expected magnitude-flux correlation from Eq. (26) takes the following form:

$$\langle \mathcal{E}_{\delta m \delta_f}(\chi) \rangle = g(\chi) A, \tag{C1}$$

where $g(\chi)$ is a function of χ (distance to absorption), and A represents the amplitude of this correlation, which one can equate with $P_{fm}(k_\parallel = 0)$ if one wishes (the precise choice will have no bearing on the final signal to noise of interest). We have suppressed the dependence on χ_Q (distance to quasar).

Our goal is to come up with an estimator for this amplitude A by combining the magnitude-flux correlations at different scales (χ's), and show that its error bar is given by Eq. (27). The estimator takes the form:

$$\mathcal{E}_A = \sum_{I,\chi} w^I(\chi) \delta m^I \delta_f^I(\chi), \tag{C2}$$

where the I index labels the quasar, and the sum over χ ranges over the (binned) scales of Lyman-α forest observations. Here, $\delta m^I = m^I - \bar{m}$, with $\bar{m}$ being the mean sample magnitude [see discussion around Eq. (A10)], and $w^I(\chi)$ represents a weighting of the data over quasars and absorption locations which remains to be specified. To satisfy $\langle \mathcal{E}_A \rangle = A$, we would want $w^I(\chi)$ to satisfy

$$\sum_{I,\chi} w^I(\chi) g(\chi) = 1. \tag{C3}$$

The variance of this estimator is given by

$$\langle \delta\mathcal{E}_A^2 \rangle = \sum_{I,J,\chi,\chi'} w^I(\chi) w^J(\chi') [\langle \delta m^I \delta_f^I(\chi) \delta m^J \delta_f^J(\chi') \rangle - \langle \delta m^I \delta_f^I(\chi) \rangle \langle \delta m^J \delta_f^J(\chi') \rangle]. \tag{C4}$$

Assuming the terms in [] are dominated by $\delta_{IJ} \langle \delta m^2 \rangle \times \langle \delta_f(\chi) \delta_f(\chi') \rangle$ (i.e. correlations between different quasars are weak, and that cross correlations between magnitude and δ_f are also weak compared with auto correlations), we find

$$\langle \delta\mathcal{E}_A^2 \rangle \sim \langle \delta m^2 \rangle \sum_{I,\chi,\chi'} w^I(\chi) \xi_{ff}(\chi, \chi') w^I(\chi'), \tag{C5}$$

where we have used $\xi_{ff}(\chi, \chi')$ to represent $\langle \delta_f(\chi) \delta_f(\chi') \rangle$—it should be kept in mind that this should include contributions from both the intrinsic forest fluctuations and shot noise. The shot-noise contribution makes ξ_{ff} strictly speaking a function of the quasar index I, but we will ignore it for our purpose of a crude S/N estimate.

Standard minimization technique applied to Eq. (C5) subject to the constraint Eq. (C3) gives us the minimum variance weighting:

$$w^I(\chi) = \Big[\sum_{\chi'} \xi_{ff}^{-1}(\chi, \chi') g(\chi') \Big] \Big/ \Big[\sum_{J,\chi',\chi''} g(\chi') \xi_{ff}^{-1}(\chi', \chi'') g(\chi'') \Big], \tag{C6}$$

where ξ_{ff}^{-1} is defined to be the matrix inverse of ξ_{ff} i.e. $\sum_{\chi'} \xi_{ff}^{-1}(\chi, \chi') \xi_{ff}(\chi', \chi'') = \delta_{\chi,\chi''}$. With this optimal weighting, the variance is given by

$$\langle \delta\mathcal{E}_A^2 \rangle = \frac{\langle \delta m^2 \rangle}{N_{\rm QSO}} \Big[\sum_{\chi',\chi''} g(\chi') \xi_{ff}^{-1}(\chi', \chi'') g(\chi'') \Big]^{-1}, \tag{C7}$$

where $N_{\rm QSO}$ is the number of quasars.

The signal to noise of interest is

$$\frac{S}{N} = \frac{A}{\sqrt{\delta\mathcal{E}_A^2}}, \tag{C8}$$

which after some Fourier manipulations is equivalent to Eq. (27).

Let us close by noting that in the same spirit and notation, the magnitude-flux correlation (at a given χ) has a variance of

$$\frac{\langle \delta m^2 \rangle}{N_{\rm QSO}} \xi_{ff}(\chi, \chi). \tag{C9}$$

[1] E. L. Turner, J. P. Ostriker, I. Gott, and J. Richard, Astrophys. J. **284**, 1 (1984).
[2] W. Fugmann, Astron. Astrophys. **204**, 73 (1988).
[3] R. Narayan, Astrophys. J. Lett. **339**, L53 (1989).
[4] E. Gaztanaga, Astrophys. J. **589**, 82 (2003).
[5] R. Scranton *et al.* (SDSS Collaboration), Astrophys. J. **633**, 589 (2005).
[6] B. Menard, R. Scranton, M. Fukugita, and G. Richards, Mon. Not. R. Astron. Soc. **405**, 1025 (2010).
[7] A. A. Meiksin, Rev. Mod. Phys. **81**, 1405 (2009).
[8] P. A. Thomas and R. L. Webster, Astrophys. J. **349**, 437 (1990).
[9] B. Ménard, Astrophys. J. **630**, 28 (2005).
[10] M. Bartelmann and A. Loeb, Astrophys. J **457**, 529 (1996).
[11] B. Menard and C. Peroux, Astron. Astrophys.**410**, 33 (2003).
[12] B. Ménard, D. Nestor, D. Turnshek, A. Quider, G. Richards, D. Chelouche, and S. Rao, Mon. Not. Roy. Astron. Soc.**385**, 1053 (2008).
[13] A. Vallinotto, S. Das, D. N. Spergel, and M. Viel, Phys. Rev. Lett. **103**, 091304 (2009).
[14] A. Vallinotto, M. Viel, S. Das, and D. N. Spergel, arXiv:0910.4125.
[15] L. Hui and E. Gaztanaga, Astrophys. J. **519**, 622 (1999).
[16] J. M. Bardeen, J. R. Bond, N. Kaiser, and A. S. Szalay, Astrophys. J. **304**, 15 (1986).
[17] N. Sugiyama, Astrophys. J. Suppl. Ser. **100**, 281 (1995).
[18] J. A. Peacock and S. J. Dodds, Mon. Not. Roy. Astron. Soc. **280**, L19 (1996).
[19] V. Springel and L. Hernquist, Mon. Not. Roy. Astron. Soc. **339**, 289 (2003).
[20] V. Springel and L. Hernquist, Mon. Not. Roy. Astron. Soc. **333**, 649 (2002).
[21] V. Springel, N. Yoshida, and S. D. M. White, New Astron. Rev. **6**, 79 (2001).
[22] V. Springel and L. Hernquist, Mon. Not. Roy. Astron. Soc. **339**, 312 (2003).
[23] N. Katz, D. H. Weinberg, and L. Hernquist, Astrophys. J. Suppl. Ser. **105**, 19 (1996).
[24] L. Hernquist, N. Katz, D. H. Weinberg, and J. Miralda-Escude, Astrophys. J. **457**, L51 (1996).
[25] C. A. Faucher-Giguere, J. X. Prochaska, A. Lidz, L. Hernquist, and M. Zaldarriaga, arXiv:0709.2382.
[26] K. Nagamine, R. Cen, L. Hernquist, J. P. Ostriker, and V. Springel, Astrophys. J. **627**, 608 (2005).
[27] P. McDonald *et al.* (SDSS Collaboration), Astrophys. J. Suppl. Ser. **163**, 80 (2006).
[28] D. N. Limber, Astrophys. J. **119**, 655 (1954).
[29] M. LoVerde and N. Afshordi, Phys. Rev. D **78**, 123506 (2008).
[30] M. Bernardi *et al.* (SDSS Collaboration), Astron. J. **125**, 32 (2003).
[31] T. S. Kim, J. S. Bolton, M. Viel, M. G. Haehnelt, and R. F. Carswell, Mon. Not. Roy. Astron. Soc. **382**, 1657 (2007).
[32] P. McDonald *et al.*, Astrophys. J. **543**, 1 (2000).
[33] V. Desjacques, A. Nusser, and R. K. Sheth, Mon. Not. Roy. Astron. Soc. **374**, 206 (2007).
[34] G. D. Becker, M. Rauch, and W. L. W. Sargent, Astrophys. J. **662**, 72 (2007).
[35] A. Lidz, K. Heitmann, L. Hui, S. Habib, M. Rauch, and W. L. W. Sargent, Astrophys. J. **638**, 27 (2006).
[36] L. Kofman, E. Bertschinger, J. M. Gelb, A. Nusser, and A. Dekel, Astrophys. J. **420**, 44 (1994).
[37] P. Coles and B. Jones, Mon. Not. R. Astron. Soc. **248**, 1 (1991).
[38] L. Hui *et al.*, Astrophys. J. **552**, 15 (2001).
[39] Sloan Digital Sky Survey III, http://www.sdss3.org/.
[40] D. J. Schlegel *et al.*, arXiv:0904.0468.
[41] K. Abazajian and L. Hui "The Lyman-alpha Forest Power Spectrum from SDSS" (unpublished).
[42] P. Zhang and P. S. Corasaniti, Astrophys. J. **657**, 71 (2007).
[43] B. Menard, T. Hamana, M. Bartelmann, and N. Yoshida, Astron. Astrophys. **403**, 817 (2003).
[44] P. McDonald, U. Seljak, R. Cen, P. Bode, and J. P. Ostriker, Mon. Not. Roy. Astron. Soc. **360**, 1471 (2005).
[45] J. F. Hennawi and J. X. Prochaska, Astrophys. J. **655**, 735 (2007).
[46] P. McDonald and D. Eisenstein, Phys. Rev. D **76**, 063009 (2007).
[47] L. Hui, E. Gaztanaga, and M. LoVerde, Phys. Rev. D **76**, 103502 (2007).
[48] L. Hui, E. Gaztanaga, and M. LoVerde, Phys. Rev. D **77**, 063526 (2008).
[49] N. Y. Gnedin and L. Hui, Mon. Not. Roy. Astron. Soc. **296**, 44 (1998).
[50] M. Zaldarriaga, L. Hui, and M. Tegmark, arXiv:astro-ph/0011559.
[51] R. Scoccimarro and J. A. Frieman, Astrophys. J. **520**, 35 (1999).